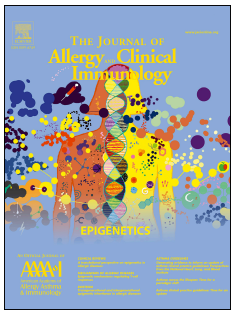
Accepted Manuscript



EMSY expression affects multiple components of skin barrier with relevance to atopic dermatitis

Martina S. Elias, PhD, Sheila C. Wright, HNC, Judit Remenyi, PhD, James C. Abbott, PhD, Susan E. Bray, PhD, Christian Cole, PhD, Sharon Edwards, MBChB, Marek Gierlinski, PhD, Mateusz Glok, John A. McGrath, FRCP, William V. Nicholson, PhD, Lavinia Paternoster, PhD, Alan R. Prescott, PhD, Sara Ten Have, PhD, Phillip D. Whitfield, PhD, Angus I. Lamond, PhD, Sara J. Brown, FRCPE

PII: S0091-6749(19)30741-9

DOI: https://doi.org/10.1016/j.jaci.2019.05.024

Reference: YMAI 14022

To appear in: *Journal of Allergy and Clinical Immunology*

Received Date: 12 March 2019

Revised Date: 7 May 2019

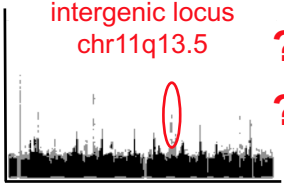
Accepted Date: 14 May 2019

Please cite this article as: Elias MS, Wright SC, Remenyi J, Abbott JC, Bray SE, Cole C, Edwards S, Gierlinski M, Glok M, McGrath JA, Nicholson WV, Paternoster L, Prescott AR, Have ST, Whitfield PD, Lamond AI, Brown SJ, *EMSY* expression affects multiple components of skin barrier with relevance to atopic dermatitis, *Journal of Allergy and Clinical Immunology* (2019), doi: https://doi.org/10.1016/j.jaci.2019.05.024.

This is a PDF file of an unedited manuscript that has been accepted for publication. As a service to our customers we are providing this early version of the manuscript. The manuscript will undergo copyediting, typesetting, and review of the resulting proof before it is published in its final form. Please note that during the production process errors may be discovered which could affect the content, and all legal disclaimers that apply to the journal pertain.

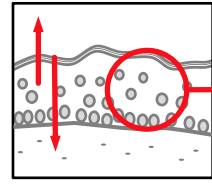
EMSY expression affects multiple components of skin barrier with relevance to atopic dermatitis (AD)

AD GWAS results → *EMSY* knockdown in skin organoid → enhancement of multiple aspects of skin barrier

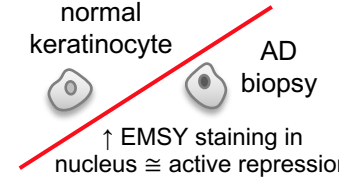


? *EMSY*

? molecular mechanisms



Assessments
- biochemical
- structural
- functional



EMSY is a **transcriptional regulator in keratinocytes** → epidermal barrier formation

ACCEPTED MANUSCRIPT

EMSY expression affects multiple components of skin barrier with relevance to atopic dermatitis

Martina S Elias PhD[1]*, Sheila C Wright HNC[1], Judit Remenyi PhD[1], James C Abbott PhD[2], Susan E Bray PhD[3], Christian Cole PhD[2], Sharon Edwards MBChB[4], Marek Gierlinski PhD[2], Mateusz Glok[1], John A McGrath FRCP[5], William V Nicholson PhD[1], Lavinia Paternoster PhD[6], Alan R Prescott PhD[7], Sara Ten Have PhD[8], Phillip D Whitfield PhD[9], Angus I Lamond PhD[8] and Sara J Brown FRCPE[1,10]*

[1] Skin Research Group, Division of Molecular and Clinical Medicine, School of Medicine, University of Dundee, Dundee, Scotland, UK

[2] Data Analysis / Bioinformatics Group, School of Life Sciences, University of Dundee, Dundee, Scotland, UK

[3] NHS Research Scotland Biorepository Tayside, Ninewells Hospital and Medical School, University of Dundee, Dundee, Scotland, UK

[4] Department of Pathology, Ninewells Hospital and Medical School, Dundee, Scotland, UK

[5] St John's Institute of Dermatology, King's College London (Guy's Campus), London, UK

[6] MRC Integrative Epidemiology Unit, Population Health Sciences, Bristol Medical School, University of Bristol, Bristol, UK

[7] Dundee imaging Facility, School of Life Sciences, University of Dundee, Dundee, Scotland, UK

[8] Centre for Gene Regulation and Expression, School of Life Sciences, University of Dundee, Dundee, Scotland, UK

[9] Lipidomics Research Facility, Division of Biomedical Sciences, University of the Highlands and Islands, Inverness, Scotland, UK

[10] Department of Dermatology, Ninewells Hospital, Dundee, Scotland, UK

ACCEPTED MANUSCRIPT

ACCEPTED MANUSCRIPT

***Co-corresponding authors**

Dr MS Elias,
Skin Research Group,
Division of Molecular & Clinical Medicine,
School of Medicine,
University of Dundee,
Dundee,
Scotland, UK
Tel: +44 (0)1382 383681
m.elias@dundee.ac.uk

Prof SJ Brown,
Skin Research Group,
Division of Molecular & Clinical Medicine,
School of Medicine,
University of Dundee,
Dundee,
Scotland, UK
Tel: +44 (0)1382 383210
s.j.brown@dundee.ac.uk

COI statement

The authors do not have any financial interests that represent a conflict of interest.

Funding

This work was funded by a Wellcome Trust Senior Research Fellowship in Clinical Science, awarded to SJB (ref 106865/Z/15/Z); the Brown laboratory has also received financial support from the Manknell Charitable Trust and the Tayside Dermatology Research Charity. LP is supported by an Academy of Medical Sciences Springboard award, which is supported by the Wellcome Trust, the Government Department for Business, Energy and Industrial Strategy, the Global Challenges Research Fund and the British Heart Foundation [SBF003\1094]; LP works in the MRC Integrative Epidemiology Unit, which receives funding from the UK Medical Research Council (MC_UU_00011/1). The mass spectrometry proteomic analysis was supported by grants to AIL from the Wellcome Trust (105024/Z/14/Z, 108058/Z/15/Z). Dundee Imaging Facility is supported by a Wellcome Trust Technology Platform award (097945/B/11/Z). UHI Lipidomics Research Facility acknowledges the support of European Regional Development Fund, Scottish Funding Council and Highlands and Islands Enterprise.

ACCEPTED MANUSCRIPT

ABSTRACT

Background

Atopic dermatitis (AD) is a common, complex and highly heritable inflammatory skin disease. Genome-wide association studies (GWAS) offer opportunities to identify molecular targets for drug development. A risk locus on chromosome 11q13.5 lies between two candidate genes - *EMSY* and *LRRC32* - but the functional mechanisms affecting risk of AD remain unclear.

Objectives

To apply a combination of genomic and molecular analytical techniques to investigate which genes are responsible for genetic risk at this locus and to define mechanisms contributing to atopic skin disease.

Methods

Interrogation of available genomic and chromosome conformation (Hi-C) data in keratinocytes; siRNA-mediated knockdown in skin organotypic culture and functional assessment of barrier parameters; mass-spectrometry global proteomic analysis and quantitative lipid analysis; electron microscopy of organotypic skin and immunohistochemistry of human skin samples.

Results

Genomic data indicate active promoters in the GWAS locus and upstream of *EMSY*; *EMSY, LRRC32* and the intergenic variants may all be within a single topologically associating domain. siRNA-knockdown of *EMSY* in organotypic culture leads to enhanced development of barrier function, reflecting increased expression of structural and functional proteins, including filaggrin and filaggrin-2, as well as long-chain ceramides. Conversely, over-expression of *EMSY* in keratinocytes leads to a reduction in markers of barrier formation. Skin biopsy samples from patients with AD show greater EMSY staining in the nucleus, consistent with increased functional effect of this transcriptional control protein.

Conclusion

Our findings demonstrate an important role for *EMSY* in transcriptional regulation and skin barrier formation, supporting EMSY inhibition as a therapeutic approach.

ACCEPTED MANUSCRIPT

Key messages

- Genetic risk loci offer the opportunity for insight into the aetiology of complex disease, but the mechanisms require detailed molecular investigation
- The atopic dermatitis-associated locus on chromosome 11q13.5 lies between two candidate genes: *EMSY* and *LRRC32*
- Our genetic, proteomic and immunohistological analyses have together demonstrated a role for EMSY expression in the control of skin barrier formation and function, of importance in atopic dermatitis
- EMSY therefore represents a future therapeutic target in atopic disease

Capsule summary

Atopic dermatitis (AD) is highly heritable but molecular mechanisms require detailed investigation. A combination of genomic data, *in vitro* modelling and clinical biopsies, demonstrate that *EMSY* plays a role in skin barrier formation of relevance to AD.

Key words

Atopic dermatitis; atopic eczema; EMSY; filaggrin; genetics; genomics; organotypic; lipidomics; proteomics; siRNA knockdown

ACCEPTED MANUSCRIPT

ACCEPTED MANUSCRIPT

Abbreviations

AD	Atopic dermatitis (synonymous with atopic eczema, or eczema)
Chr	Chromosome
EMSY	Gene encoding the EMSY protein
ENCODE	Encyclopaedia of DNA elements
eQTL	Expression quantitative trait locus
ExAC	Exome aggregation consortium
GO	Gene ontology
GWAS	Genome-wide association study
Hi-C	Genome-wide chromosome conformation capture and high throughput sequencing to identify regions of DNA showing interaction in 3-dimensional space
HGNC	Human Genome Nomenclature Committee
NHK	Normal human keratinocytes
NDF	Normal dermal fibroblasts
NT	Non-targeting
LRRC32	Leucine-rich repeat-containing 32, gene encoding GARP (glycoprotein A repetitions predominant) protein
siRNA	Small interfering RNA
SNP	Single nucleotide polymorphism
TEWL	Transepidermal water loss

ACCEPTED MANUSCRIPT

INTRODUCTION

Atopic dermatitis (AD, or eczema[1]) is a common inflammatory skin disease with strong heritability.[2] Genome-wide association studies (GWAS) have identified multiple loci affecting AD risk[3] including effects on skin barrier and immune function[2, 4] and it has been demonstrated in other complex traits that molecular mechanisms defined by GWAS loci may represent effective therapeutic targets.[5]

The most widely replicated genetic risk for AD lies within the epidermal differentiation complex on chromosome 1q21.3;[3, 6, 7] this includes *FLG,* encoding the skin barrier protein filaggrin.[8] The expression levels of filaggrin and its metabolites in the outer epidermis correlate with AD activity.[9, 10] However, this mechanism has not been successfully targeted in therapy development since its discovery more than 10 years ago.

An association peak within an intergenic region on chromosome 11q13.5 was identified in the earliest AD GWAS.[6] This locus has been replicated in subsequent GWAS[11-13] and meta-GWAS.[3, 7] In addition to AD, the region is associated with multiple atopic phenotypes[14, 15] and other disorders characterized by epithelial barrier dysfunction, including polyallergen sensitization,[14, 16] asthma,[17] allergic rhinitis,[18] food allergy,[19, 20] eosinophil count,[21] eosinophilic oesophagitis,[22] inflammatory bowel disease[23] and the gut microbiome.[24] The AD-associated single nucleotide polymorphisms (SNPs) are in an intergenic region between *LRRC32* and *EMSY. LRRC32* encodes transforming growth factor beta activator LRRC32 (leucine-rich repeat-containing 32, previously termed GARP (glycoprotein-A repetitions-predominant) UniProtKB Q14392). This is a membrane protein that binds latent TGF-beta-1 on the surface of activated regulatory T-cells.[25] *LRRC32* has been proposed as a causal gene for atopic skin inflammation,[26] but the credible SNPs identified by GWAS at this locus are all intergenic,[3] suggesting that regulatory rather than coding variants drive the association. *EMSY,* also known as BRCA2-interacting transcriptional repressor and previously termed *C11orf30,* codes for a protein EMSY (UniProtKB Q7Z589) that is expressed in multiple human tissues, including cerebellum, breast, lung, ovary, uterus and skin (GTEx RNA-seq, V7). EMSY has been characterized as a transcriptional regulator, either repressing transcription as part of a chromatin remodelling complex or activating transcription as part of a histone H3-specific methyltransferase complex.[27] *EMSY* amplification is associated with DNA damage and increased risk of malignancy in breast and ovarian tissue.[27] EMSY may also play a role in

inflammation, since the protein kinase AKT1 regulates the interferon response through phosphorylation of EMSY,[28] but its role in skin remains undefined.

We set out to investigate, using genetic and genomic data, whether *EMSY* and/or *LRRC32* showed evidence of activity in human skin cells. We then investigated the mechanism of effect by functional and multi-omic analysis of organotypic skin, followed up with immunostaining of AD biopsy samples.

METHODS

Human tissues and cells

All human tissues were obtained with written informed consent from donors, under the governance and with ethical approval, from the NHS Research Scotland Biorepository in Tayside. Primary keratinocytes and donor-matched primary fibroblasts were extracted from skin samples discarded from plastic surgical procedures. AD skin samples were identified from the hospital pathology database, as consecutive unselected cases. Demographic details are in the online repository.

Cell and skin organotypic culture

Normal human keratinocytes (NHK) and normal dermal fibroblasts (NDF) were isolated from healthy breast skin by sequential collagenase D and trypsin EDTA digestion, as previously described.[29] NHKs were co-cultured in RM media (3:1 DMEM : Hams F12, 10% FCS, 0.4µg/ml hydrocortisone, 5µg/ml insulin, 10ng/ml EGF, 5µg/ml transferrin, 8.4ng/ml cholera toxin and 13ng/ml liothyronine) (Sigma Aldrich, Gillingham, Dorset, UK) along with mitomycin C inactivated 3T3 feeder cells.[30] Epidermal growth factor (EGF) was omitted for the first day of culture. NDFs were cultured in DMEM supplemented with 10% FCS under standard conditions.

Fibrin gel dermal equivalents were prepared using a protocol adapted from published methods.[31-33] 0.5ml fibrinogen (35 mg/ml in NaCl) (Sigma Aldrich, Gillingham, Dorset, UK) and 0.5ml thrombin (3U/ml in 2 mM $CaCl_2$ / 1.1% NaCl) (Sigma Aldrich, Gillingham, Dorset, UK) were combined on ice, supplemented with 200,000 NDFs, aprotinin (0.1 U/ml) (Sigma Aldrich, Gillingham, Dorset, UK) and transferred to a 12-well plate. Following 30 minutes incubation at 37^{o}C the gels were covered in medium (DMEM, 10% FCS, 0.1 U/ml Aprotinin) and cultured overnight (day 1). The following day the medium was replaced with RM medium excluding EGF, 0.1U/ml aprotinin and 2 x 10^6 suspended NHKs (day 2). This was refreshed daily for the next two days (day 3 and 4) with RM medium containing 0.1ng/ml EGF and 0.1U/ml aprotinin. On day 5 gels were carefully removed from wells using a plastic spatula and lifted onto custom-made steel grids lined with nylon gauze (Millipore, Livingston, Scotland, UK). RM medium supplemented with 0.1ng/ml EGF and 0.1U/ml aprotinin was

added up to the base of the grid enabling the fibrin gels to be nourished from below and the epidermis cultured at the air-liquid interface. Medium was refreshed every other day until day 12 when the cultures were analysed. Where required the epidermis was isolated from the fibrin gel following hypertonic saline-induced split (4 hours, 1M NaCl, 4^{o}C).

siRNA mediated knockdown

NHKs were reverse transfected immediately prior to inclusion in the organotypic cultures using RNAiMax transfection reagent (Life Technologies, Carlsbad, California, USA) according to manufacture's instructions. Briefly, siRNA complexes were formed in OPTIMEM medium (20uM siRNA, 5µl RNAiMAX) and following 20 minutes incubation, combined with 2 x 10^6 suspended NHKs and transferred to the pre-prepared dermal substrate. A pool of 4 siRNA duplexes was used [EMSY: LQ-004081-00-0002, FLG: LQ-021718-00-0002, Control: ON-TARGETplus non-targeting siRNA #4 D.001810-04-20] (Dharmacon, Lafayette, Colorado, USA).

***EMSY* overexpression in primary keratinocytes**

A second generation lentiviral system was used, as follows: Pseudoviral particles were prepared using psPAX2 packaging (CAT#: 12260; AddGene, Watertown, Massachusetts, USA) and pMD2.G plasmid (CAT#: 12259; AddGene, Watertown, Massachusetts, USA) which were co-transfected with the control pLenti-C-mGFP-P2A-puromycin tagged cloning vector (CAT#: PS100093; OriGene, Rockville, Maryland, USA) plasmid or with the Lenti-ORF clone of mGFP-tagged-human chromosome 11 open reading frame 30 (*C11orf30*) (CAT#: RC216916L4; OriGene, Rockville, Maryland, USA) plasmid using Lipofectamine-3000TM transfection reagent (CAT#: L3000008, Invitrogen, Carlsbad, California, USA) following the manufacturer's protocol into 293T packaging cells for 16h. Next morning the cells were washed twice with PBS to remove excess plasmid DNA and the media was replaced with virus producing media (20% FBS/DMEM). 48h, 72h and 96h after the transfection the 1st, 2nd and 3rd virus supernatants were harvested. Virus supernatant was spin down at 1200rpm for 15 minutes and filtered using a 0.45µm filter.

Primary human keratinocytes from donor skin were transduced twice: First in RM media without EGF; after treating the keratinocytes with trypsin, 1x10^6 cells/well were mixed with 10µg/ml Polybrene (hexadimethrine bromide; CAT#: H9268, Sigma Aldrich, Gillingham, Dorset, UK) and 1 or 2ml of virus supernatant then plated onto 6-well plates and cultured overnight. The second transduction was performed in monolayer culture, using RM media without EGF, 10 µg/ml Polybrene and 1 or 2ml of virus supernatant. Cells were incubated for 90 minutes at 37^{o}C followed by centrifugation at 1200rpm. To eliminate excess virus, cells were washed twice with PBS and the media replaced by RM media (3:1 DMEM : Hams F12, 10% FCS, 0.4µg/ml hydrochortisone, 5µg/ml insulin, 10ng/ml EGF, 5µg/ml transferrin, 8.4ng/ml cholera toxin and 13ng/ml liothronine). Fresh RM

media was replaced every second day and samples were harvested on day 10 after transduction as a differentiated culture.

Fluorescent dye penetration

50µl of 1mM lucifer yellow dye (Sigma Aldrich) was added to the epidermal surface of the organotypic and incubated at 37^{o}C for 4 hours. Metal cloning rings were used to control uniform dosing on the epidermal surface. The lucifer yellow was removed and the organotypics washed in PBS before formalin fix-paraffin embedding under standard conditions. 4µM sections were deparaffinized, counterstained with DAPI (1µg/ml for 10 mins) (Life Technologies, Carlsbad, California, USA) and imaged by confocal Zeiss LSM710 microscope. Quantification of dye penetration in the upper dermis (average intensity in upper 40µm) was performed using Zeiss Zen software and compared using paired t-tests.

Transepidermal water loss

Organotypic cultures were equilibrated at room temperature and atmospheric conditions for 30 minutes before transepidemal water loss (TEWL) was measured at 2 locations on the epidermal surface using an Aquaflux AF200 instrument (Biox Systems Ltd, London, UK) with a custom (5mm diameter) probe head. TEWL measurements were taken every second for a minimum of 60 seconds until a stable reading, as determined by the software, was obtained.

Capacitance

Organotypic cultures were equilibrated at room temperature and atmospheric conditions for 30 minutes prior to measurement of epidermal surface capacitance, as a measure of water content, using a Corneometer^{TM} (Courage and Khazaka, Cologne, Germany). Three measurements were recorded from each organotypic and the mean was calculated.

Protein data analysis

Network analysis was performed using Ingenuity Pathway Analysis, (Qiagen Ingenuity version 01-12). Gene Ontology enrichment analysis was performed in the Gene Ontology Consortium online tool using PANTHER classification http://www.geneontology.org/page/go-enrichment-analysis (accessed 28 August 2018). A volcano plot was generated in R/ggplot2 using human proteins detected in all 4 of the replicates to calculate the fold change (non-targeting control/EMSY knockdown) for each donor with $\log_{10}$ transformation and t-test for significance.

Lipid staining

Frozen sections of skin organotypic samples were cut and air-dried onto slides before formalin fixation and rinse with 60% isopropranol. Oil Red O (Sigma Aldrich, Gillingham, Dorset, UK) working

solution was freshly prepared and sections were stained for 15 minutes, rinsed with 60% isopropanol then lightly counter-stained with alum haematoxylin before a final rinse with distilled water.

Additional Methods are described in the Online Repository.

RESULTS

Genomic data support EMSY *and* LRRC32 *as candidate genes in skin*

The AD-associated SNPs at the chromosome 11q13.5 locus are approximately 27kb downstream of *EMSY* (HGNC:18071, ENSG00000158636) and ~77kb downstream of *LRRC32* (HGNC:137207, ENSG00000137507). The credible set identified by mapping this locus lies entirely within an intergenic region (**Fig 1**). ENCODE and Ensembl data predict multiple regulatory features within the region of disease risk SNPs and there are putative promoters upstream of each gene (**Fig 1**). Focussing on skin, there are histone H3K27ac marks indicating active enhancers or promoters in normal human keratinocytes in the AD risk locus and at the 3' end of *EMSY,* but not *LRRC32* (**Fig 1**).

Enhancer-promoter interactions may occur by proximity in three-dimensional space[34] and show cell lineage-specificity;[35] we therefore re-analysed two sets of genome-wide chromosome conformation capture (Hi-C) data generated from normal human keratinocytes. Interrogation of Hi-C data[36] shows that the intergenic SNPs, *EMSY* and *LRRC32* all lie within a single topologically associated domain in keratinocytes (**Fig E1**), supporting a possible functional interaction. Analysis of promoter-capture Hi-C[37] in differentiating keratinocytes showed evidence of interaction between the promoter region of *LRRC32* and the intergenic SNP locus, but these data were not sufficiently detailed to determine whether or not *EMSY* also shows conformational interaction (**Fig E1**).

Gene expression data[38] and our own single molecule RNA sequencing analysis[39] confirm expression of each gene in skin, but there is no significant difference in *EMSY* or *LRRC32* mRNA abundance in atopic skin compared to non-atopic control skin ($p>0.05$, Fig E2). However *EMSY* is more highly expressed in skin than *LRRC32* at the protein level (https://www.proteinatlas.org/) and it has not previously been studied in keratinocyte biology; *EMSY* was therefore selected for further detailed investigation.

EMSY knockdown in a skin organotypic model enhances barrier function

To investigate a functional effect of EMSY in skin we used primary human keratinocytes seeded onto a dermal equivalent, which forms an organotypic model with stratified layers that effectively recapitulate the structure and gene expression patterns of human skin.[40] The model also demonstrates functional parameters controlling the entry and exit of small molecules and this can be used to quantify effects on barrier formation and function.[41] siRNA knockdown of *EMSY* expression was achieved by transfection of keratinocytes immediately prior to seeding onto the dermal equivalent. Knockdown was confirmed at mRNA and protein level, persisting to 10 days in organotypic culture (**Fig 2A-C**). Equivalent effects were seen using individual and pooled siRNAs (**Fig E3**). EMSY knockdown produced a marked phenotypic change (**Fig 2D**), including thickening of the epidermal cell layer and stratum corneum (**Fig 2E**). There was an increase in the number of layers within the stratum corneum and frequency of corneodesmosomes (**Fig 2F**). The stratum granulosum, the site of filaggrin expression,[8] was also more prominent (**Fig 2D**) and increased filaggrin expression was confirmed by qPCR (n=7 replicates, mean ± SEM fold-change 2.00±0.41 compared to non-targeting control) and Western blotting (n=7, mean fold-change 1.97±0.22) (**Fig 2G**).

In our skin culture model, stratum corneum hydration, transepidermal water loss (TEWL) and lucifer yellow dye penetration progressively decrease as the skin barrier is formed (**Fig E4**). EMSY knockdown in the skin model resulted in a reduction in stratum corneum hydration (**Fig 3A**), a reduction in TEWL (**Fig 3B**) and a reduction in penetration of the lucifer yellow dye (**Fig 3C** and **Fig 3D**), in keeping with enhanced and accelerated barrier development compared to control siRNA treatment.

EMSY over-expression reduces filaggrin expression

In contrast to the phenotype observed with *EMSY* knockdown, over-expression of *EMSY* in primary human keratinocytes resulted in a reduction of multiple markers of differentiation and barrier formation at mRNA and protein level (**Fig 4 A-D** and **Fig E5**).

Proteomic analysis reveals pathways inhibiting the development of dermatitis

To assess in more detail the EMSY knockdown phenotype, we applied tandem mass spectrometry (MS/MS) global proteomic analysis to donor-matched control and EMSY-knockdown organotypic experiments from 4 independent donors. Total epidermal protein

extracts were fractionated using high pH reversed phase chromatography before MS/MS analysis, which identified over 9000 proteins per sample (**Fig E6**). qPCR and Western blotting confirmed knockdown of EMSY in each sample. A greater proportion of proteins showed increased rather than decreased expression upon EMSY knockdown (**Fig 5A**) indicating that EMSY's predominant role is as a transcriptional repressor in this tissue.

Data were filtered for proteins showing changes in the same direction consistently across all four biological replicates, and fold change of ≥2.5 (n=154 proteins) or ≤0.5 (n=130 proteins) in at least three out of four of the biological replicates. Consistent direction of change was used as a criterion to focus analysis on changes of relevance to EMSY knockdown and showing reproducibility across different donors, to minimize any effect of inter-individual differences.

Gene ontology (GO) analysis of the up-regulated proteins showed enrichment for the biological processes termed: establishment of skin barrier (GO:0061436); skin development (GO:0043588); regulation of water loss via skin (GO:0033561) and cornification (GO:0070268) (each FDR p≤0.037). GO analysis of the down-regulated proteins showed enrichment of cellular components termed: cytosol (GO:0005829); mitochondrial membrane (GO:0031966) and golgi membrane (GO:0000139) (each FDR p≤0.010). The full lists of GO terms defined by this analysis are shown in **Fig E7**.

Pathway analysis (Ingenuity version 01-12, Qiagen) identified up-regulation of pathways predicted to inhibit the development of dermatitis and ichthyosis (**Fig 5B**). The differential expression levels of proteins from these pathways were tested for validation using qPCR, Western blotting and/or immunostaining of organotypic skin. All positive and negative findings, and untested proteins, are displayed in **Fig E8**.

EMSY knockdown increases long chain ceramides

Organotypic samples showed an increase in abundance of epidermal lipid staining with EMSY knockdown (**Fig 6A**) in keeping with the increase in proteins involved with lipid metabolism (*e.g*. STS, ALOXE3, ALOX12B and APOE). Mass spectrometry lipid analysis showed an increase in long-chain ceramides and esterified omega-hydroxy-ceramides species in organotypic samples with EMSY knockdown (**Fig 6B**); these are the ceramides which have previously been reported to show a reduction in AD skin samples.[42]

EMSY knockdown increases cell-cell adhesion structures

Ultrastructural analysis demonstrated an increase in size of desmosomes (**Fig 6C**) consistent with the observed increase in desmocollin 1. An increase in the number of layers within the stratum corneum was also observed, consistent with the increase in corneodesmosin (**Fig 2F** and **Fig E9**).

EMSY shows predominantly nuclear localisation in skin affected by AD

To investigate the expression of EMSY in human skin samples, we compared 18 normal control skin samples and biopsies from 14 patients with spongiotic dermatitis and/or AD. Immunohistochemistry showed considerable inter-individual variability in EMSY staining, despite careful standardization of staining conditions, and there was no consistent difference in the total intensity between cases and controls (**Fig E10**). However, all 14 AD cases showed greater nuclear than cytoplasmic staining and 12/14 (86%) of cases showed predominantly nuclear staining extending throughout the epidermis compared to 2/18 (11%) controls (example images shown in **Fig 7**; all images in **Fig E10**). Similarly, the control organotypic sample showed EMSY staining in nuclei throughout the epidermis, whilst the organotypic with EMSY knockdown showed expression predominantly in the basal epidermis in keratinocyte nuclei. Thus increased nuclear expression is consistent with increased activity of EMSY as a transcriptional regulator within keratinocytes in AD lesional skin.

DISCUSSION

Genome-wide association studies have provided valuable insight into the pathogenic mechanisms of many common complex traits, and some have been exploited for targeted therapy development.[5, 43, 44] However, many of the loci identified by GWAS are intergenic and the molecular mechanisms require detailed functional analysis, performed in disease-relevant tissue, to characterize important pathomechanisms.[45] Increasing understanding of the regulatory features in intergenic DNA[46, 47] provides insight into possible effector genes, either locally or distant from variants identified by GWAS. Skin as an organ that can be cultured *in vitro* offers an opportunity to investigate genetic mechanisms using primary cells, quantification of barrier function and detailed molecular analyses. Cells extracted from normal human skin have been used in our model to investigate the effect of a single

candidate gene, without the multiple genetic and epigenetic effects that would be co-inherited in cells harvested from an AD patient.[2] The use of primary cells more closely represents skin physiology than an immortalized cell line and replication in multiple donors is used to control for inter-individual variation.

Our findings from genomic data, *in vitro* and *ex vivo* analyses converge to provide an understanding of the role of EMSY in skin barrier function. The epigenetic regulatory mechanisms indicated by methylation and chromosomal confirmation (**Fig 1**) provide a possible mechanism by which the intergenic SNPs associated with AD may affect EMSY expression. However, additional epigenetic mechanisms,[48] including other forms of histone modification, micro RNAs and long non-coding RNAs, may also play roles in EMSY transcriptional control. The greater nuclear localisation of EMSY in AD lesional skin indicates increased activity of this transcriptional repressor. This is in keeping with our findings in primary cell culture, where EMSY over-expression leads to a reduction in multiple proteins that have previously been shown to be biomarkers for AD.[49-51] Improvements in analytical capacity have increased understanding of the importance of lipid composition in epidermal physiology and pathophysiology including atopic disease,[52] and the observed increase in relevant lipid species emphasizes the role of EMSY in controlling multiple aspects of skin barrier function.

It is interesting to note that EMSY knockdown increases filaggrin expression whilst EMSY over-expression leads to a marked reduction in profilaggrin. This may in part explain the observation that the genetic risk variants in chr11q13.5 and *FLG* show a multiplicative effect in population analysis.[53] Chr11q13.5 and the *FLG* locus also both show their strongest associations within a subgroup of early onset and persistent AD in childhood,[54] in keeping with their combined effect leading to a more severe phenotype.

EMSY loss-of-function mutations are rare: they are detected in 1/60,000 unrelated individuals in ExAC;[55] the minor allele frequency is approximately 0.001 in the Exome Variant Server;[56] and there are no homozygous loss-of-function genotypes identified in gnomAD.[57] This is consistent with our finding that even a modest reduction in expression (mean ~33% reduction in mRNA or protein in our experimental model) results in a marked phenotypic change in organotypic culture. Together these observations indicate that loss-of-function mutations are likely to have a deleterious effect and more subtle modulation of EMSY

411 expression is required for optimal skin barrier function. It is therefore tempting to speculate
412 that the control of filaggrin expression and skin barrier function via EMSY may be a more
413 sensitive mechanism to exploit than targeting filaggrin directly. It may also be a more
414 tractable target, since the therapeutic effect would be achieved by knockdown (of EMSY)
415 rather than attempting to increase expression (of filaggrin).

416 Loci reaching statistical significance in genome-wide analysis may reflect the combination of
417 more than one functional association and multi-effect loci have been observed in AD as well
418 as other complex traits.[12, 58] Our finding of a role for EMSY in keratinocytes does not
419 preclude an additional effect of EMSY via expression in T cells[59] which are known to play a
420 key role in AD pathogenesis.[2] Intriguingly, immunohistochemistry also reveals EMSY staining
421 within the nuclei of cells in the dermis (**Fig 6** and **Fig E10**). This may represent an
422 inflammatory infiltrate including T cells and warrants further investigation. Similarly, the
423 genomic promoter-capture Hi-C analysis (**Fig E1**) provides more support for a possible
424 promoter-promoter interaction between the GWAS locus and *LRRC32* than *EMSY*, suggesting
425 that an effect via *LRRC32* expression in keratinocytes or T cells may also play a role in the
426 pathogenesis of AD. Further work, including high-resolution 3C,[60] could be used to finely
427 map these important regulatory interactions.

428 Expression quantitative trait locus (eQTL) analysis is an approach which has been used to
429 investigate genes responsible for risk mechanisms attributable to intergenic loci.[61] However,
430 eQTL analysis relies on the genetic variants having a quantitative effect on mRNA abundance
431 of sufficient magnitude to be detected with a suitably stringent level of statistical
432 significance.[62] Other mechanisms may affect disease risk without substantially altering the
433 total amount of mRNA, for example protein localisation at a functional site, as appears to be
434 the case for EMSY. Furthermore, EMSY has at least 7 isoforms produced by alternative
435 splicing as well as 14 annotated phosphorylation or glycosylation sites
436 (https://www.uniprot.org/uniprot/Q7Z589); it is likely that these mechanisms also
437 contribute to functional regulation in different cells and tissue types.

438 The analysis of a single cell type, the keratinocyte, at different stages of terminal
439 differentiation represents a reductionist view of the epidermis, but the skin organotypic has
440 proven to be a valuable model for the investigation of molecular mechanisms controlling
441 differentiation in this multi-layered tissue.[40, 63] A limitation to the model is that the various

dermal appendages (hair follicles, sweat glands, sebaceous glands *etc*.) are absent, as are the dermal blood vessels and neurons, although these may play a role in skin inflammation.[64, 65] Immune cells of the haematopoietic lineage are also missing from this model, but there is increasing recognition of the role of keratinocytes in immune signaling[66, 67] and the organotypic displays innate immunological mechanisms.

The work presented here has identified EMSY as a therapeutic target: knockdown *in vivo* is predicted to improve skin barrier function and protect against AD. However, considerable further work is needed, including high throughput screening to identify molecules capable of reducing the abundance of nuclear EMSY, followed by preclinical testing, before these findings can be assessed in clinical trials. The advent of biological therapy to target the immune component of AD has transformed care for patients with moderate-severe disease,[68] but therapies designed to improve skin barrier function are also required as an alternative or complimentary approach for this complex and therapeutically challenging disorder.

ACCEPTED MANUSCRIPT

FIGURES and LEGENDS

FIG 1. Regulatory features of the AD risk locus and adjacent genes on chromosome 11q13.5.
Genes (navy) flanking locus with multiple disease-associated SNPs (green) identified by GWAS; *EMSY* has a protein-coding region spanning 106kb, with 20 exons producing 18 splice variants; *LRRC32* spans 13kb including 3 exons; the location of the credible set of AD-associated SNPs[3] is marked; H3K27ac marks (pink) and DNase I hypersensitivity (grey) data from ENCODE (accessed June 2018). Regulatory features in the same region of chromosome 11, from Ensembl (GRCh38.12), accessed April 2019.

FIG 2. Biochemical and histological effects of *EMSY* knockdown in skin organotypic model *in vitro*.
(**A**) qPCR showing knockdown of *EMSY* mRNA after 10 days in culture (7 days after lifting to the air-liquid interface) normalized to non-targeting control-treated sample; n=7; mean 36% reduction compared to non-targeting control. (**B**) Western blot showing knockdown of EMSY protein after 10 days in culture and (**C**) Densitometry to quantify protein knockdown, normalised to non-targeting control; n=7. (**D**) Appearance of organotypic cultures showing increased granular layer and thickened stratum corneum in response to *EMSY* siRNA knockdown; representative images replicated in 10 independent donor experiments; scale bar 25µm. (**E**) Relative thickness of epidermal layers; n=10. (**F**) Transmission electron microscopy of stratum corneum, showing an thickness of stratum corneum (white arrow) with an increase in the number of layers and number of corneodesmosomes (black arrowheads). (**G**) Western blot showing filaggrin expression in skin organotypic cultures, untreated (mock) and treated with non-targeting siRNA, *FLG*-siRNA and *EMSY*-siRNA, 7 days after lifting to the air-liquid interface. Paired t-test **p<0.001 ***p<0.0001; NT, non-targeting control siRNA; bars show mean and standard error of mean.

FIG 3. Functional effects of *EMSY* knockdown in skin organotypic model.
(**A**) Water content of the stratum corneum measured by capacitance on the skin surface; n=5; paired t-test **p<0.001 ***p<0.0001 (**B**) Water evaporation from the epidermal surface measured as transepidermal water loss (TEWL); n=5. (**C**) Visualisation of fluorescent dye penetration through the epidermis and dermis after 4 hours, in skin organotypic cultures developed for 3, 5 and 7 days after lifting to the air-liquid interface; representative images from experiment replicated in 5 independent donor experiments; (**D)** Overexpression of EMSY in primary human keratinocytes and concomitant reduction in expression of differentiation markers; n=5.

FIG 4. Functional effects of *EMSY* knockdown in skin organotypic model.

(**A**) Overexpression of EMSY in primary human keratinocytes and concomitant reduction in expression of differentiation markers at mRNA (**B**) and protein level (**C, D**); n=3; quantification of protein blots by densitometry is shown in **Fig E5**.

FIG 5. Proteomic analysis of EMSY knockdown in skin organotypic model.

(**A**) Volcano plot showing mean fold change in four biological replicate samples comparing non-targeting control siRNA-treated model with *EMSY* siRNA knockdown; t-test results are colour-coded red P<0.05; orange fold change ≤2.5 or ≥0.5; green P<0.05 and fold change ≥2.5 or ≤0.5. (**B**) Ingenuity Pathway Analysis (Qiagen) of proteins consistently up- or down-regulated (0.5≥fold change≥2.5) in ≥3 out of 4 biological replicates, showing proteins defective in monogenic skin diseases with similarities to AD including ichthyoses[69-72], hyperkeratosis[73] or skin fragility [74, 75] (red asterisks) and an enhancement of pathways predicted to inhibit the development of dermatitis, hyperkeratosis and hair disorders (blue cogwheels).

FIG 6. Lipid and ultrastructural analyses of EMSY knockdown in skin organotypic model.

(**A**) Lipid staining of skin organotypic samples treated with non-targeting (NT) siRNA control and *EMSY* siRNA; Oil Red O stains neutral lipids. (**B**) Mass spectrometry lipid analysis showing a greater abundance of ceramides with longer chain length in *EMSY*-siRNA treated organotypic skin compared with non-targeting siRNA control; x axis, non-hydroxy fatty acid carbon chain length; n=5 biological replicate samples; lines show best fit of linear model and 95% CI (shaded areas); p-values are for the term in the linear model for lipid chain length. (**C**) Transmission electron microscopy, osmium tetroxide post-fixed and stained showing increased size of desmosomal structures (arrowed) in the *EMSY* knockdown skin model; scale bar 1µm.

FIG 7. EMSY localisation in skin with and without AD.

Immunohistochemistry showing EMSY staining in a predominantly basal distribution in normal human skin in contrast to nuclear staining extending throughout the epidermis in AD lesions; representative images are taken from a tiled image of the whole specimen viewed using Deep Zoom; scale bar ≈20µm.

Acknowledgements

We are very grateful to the anonymous skin donors who gave consent for their samples to be accessed for research under the governance of the NHS Research Scotland Biorepository Tayside. We thank Dr Andrew South, Dr Celine Pourreyron, Dr Michael Mildner and Prof Erwin Tschachler for expert advice on skin organotypic culture methods; Dr Paul Appleton for technical expertize and advice on microscopy; Dr Lynda Weir for her contributions to antibody validation; Mr Seshu Tammireddy for his technical work in lipid analysis; Dr Adam Rubin and Prof Paul Khavari for clarification of their data stored on GEO; Prof Jim Hughes and Dr Damien Downes for expert advice on Hi-C data analysis. We acknowledge Mohan Babu, University of Regina for the production, and Addgene for storage and supply of the EMSY over-expression plasmid 83480 lentiCRISPR v2-Blast.

Author contributions

MSE, SW, JR, STH, PDW, AIL and SJB have made substantial contributions to the conception or design of the work; MSE, SW, JR, JCA, CC, SE, MGi, MGl, SEB, JMcG, WN, LP, AP, STH, PDW, AIL and SJB have contributed to the acquisition, analysis, or interpretation of data; MSE, SW, JR, JCA, CC, MGi, WN, LP, AP, STH and SJB have contributed to drafting or substantively revising the manuscript. All authors have reviewed and approved the final draft of this manuscript.

Competing interests: The authors do not have any financial interests that represent a conflict of interest.

Data and materials availability: The proteomics raw data are deposited in the PRIDE proteomics data repository (https://www.ebi.ac.uk/pride/archive/); processed data are available in the Encyclopedia of Proteome Dynamics (https://www.peptracker.com/accounts/login/epd/) (accession numbers to be added on publication) and processed data in an Excel format are made available in FigShare (DOI to be added on publication). Materials are available, within ethical constraints and with an MTA, by request to the corresponding authors.

ACCEPTED MANUSCRIPT

REFERENCES

1. Johansson S, Bieber T, Dahl R, Friedmann P, Lanier B, Lockey R, et al. Revised nomenclature for allergy for global use: Report of the Nomenclature Review Committee of the World Allergy Organization, October 2003. J Allergy Clin Immunol 2004; 113:832-6.

2. Weidinger S, Novak N. Atopic dermatitis. Lancet 2016; 387:1109-22.

3. Paternoster L, Standl M, Waage J, Baurecht H, Hotze M, Strachan DP, et al. Multi-ancestry genome-wide association study of 21,000 cases and 95,000 controls identifies new risk loci for atopic dermatitis. Nat Genet 2015; 47:1449-56.

4. Brown SJ. Molecular mechanisms in atopic eczema: insights gained from genetic studies. J Pathol 2017; 241:140-5.

5. Finan C, Gaulton A, Kruger FA, Lumbers RT, Shah T, Engmann J, et al. The druggable genome and support for target identification and validation in drug development. Sci Transl Med 2017; 9.

6. Esparza-Gordillo J, Weidinger S, Folster-Holst R, Bauerfeind A, Ruschendorf F, Patone G, et al. A common variant on chromosome 11q13 is associated with atopic dermatitis. Nat Genet 2009; 41:596-601.

7. Paternoster L, Standl M, Chen CM, Ramasamy A, Bonnelykke K, Duijts L, et al. Meta-analysis of genome-wide association studies identifies three new risk loci for atopic dermatitis. Nature genetics 2011; 44:187-92.

8. Irvine AD, McLean WH, Leung DY. Filaggrin mutations associated with skin and allergic diseases. N Engl J Med 2011; 365:1315-27.

9. Winge MC, Hoppe T, Berne B, Vahlquist A, Nordenskjold M, Bradley M, et al. Filaggrin genotype determines functional and molecular alterations in skin of patients with atopic dermatitis and ichthyosis vulgaris. PLoS One 2011; 6:e28254.

10. Brown SJ, Kroboth K, Sandilands A, Campbell LE, Pohler E, Kezic S, et al. Intragenic copy number variation within filaggrin contributes to the risk of atopic dermatitis with a dose-dependent effect. J Invest Dermatol 2012; 132:98-104.

11. Schaarschmidt H, Ellinghaus D, Rodriguez E, Kretschmer A, Baurecht H, Lipinski S, et al. A genome-wide association study reveals 2 new susceptibility loci for atopic dermatitis. J Allergy Clin Immunol 2015; 136:802-6.

12. Ellinghaus D, Baurecht H, Esparza-Gordillo J, Rodriguez E, Matanovic A, Marenholz I, et al. High-density genotyping study identifies four new susceptibility loci for atopic dermatitis. Nat Genet 2013; 45:808-12.

13. Hirota T, Takahashi A, Kubo M, Tsunoda T, Tomita K, Sakashita M, et al. Genome-wide association study identifies eight new susceptibility loci for atopic dermatitis in the Japanese population. Nat Genet 2012; 44:1222-6.

14. Ferreira MA, Vonk JM, Baurecht H, Marenholz I, Tian C, Hoffman JD, et al. Shared genetic origin of asthma, hay fever and eczema elucidates allergic disease biology. Nat Genet 2017; 49:1752-7.

15. Zhu Z, Lee PH, Chaffin MD, Chung W, Loh PR, Lu Q, et al. A genome-wide cross-trait analysis from UK Biobank highlights the shared genetic architecture of asthma and allergic diseases. Nat Genet 2018.

16. Amaral AF, Minelli C, Guerra S, Wjst M, Probst-Hensch N, Pin I, et al. The locus C11orf30 increases susceptibility to poly-sensitization. Allergy 2015; 70:328-33.

17. Demenais F, Margaritte-Jeannin P, Barnes KC, Cookson WOC, Altmuller J, Ang W, et al. Multiancestry association study identifies new asthma risk loci that colocalize with immune-cell enhancer marks. Nat Genet 2018; 50:42-53.

18. Ramasamy A, Curjuric I, Coin LJ, Kumar A, McArdle WL, Imboden M, et al. A genome-wide meta-analysis of genetic variants associated with allergic rhinitis and grass sensitization and their interaction with birth order. J Allergy Clin Immunol 2011; 128:996-1005.

19. Marenholz I, Grosche S, Kalb B, Ruschendorf F, Blumchen K, Schlags R, et al. Genome-wide association study identifies the SERPINB gene cluster as a susceptibility locus for food allergy. Nat Commun 2017; 8:1056.

20. Asai Y, Eslami A, van Ginkel CD, Akhabir L, Wan M, Ellis G, et al. Genome-wide association study and meta-analysis in multiple populations identifies new loci for peanut allergy and establishes C11orf30/EMSY as a genetic risk factor for food allergy. J Allergy Clin Immunol 2018; 141:991-1001.

21. Astle WJ, Elding H, Jiang T, Allen D, Ruklisa D, Mann AL, et al. The Allelic Landscape of Human Blood Cell Trait Variation and Links to Common Complex Disease. Cell 2016; 167:1415-29 e19.

22. Sleiman PM, Wang ML, Cianferoni A, Aceves S, Gonsalves N, Nadeau K, et al. GWAS identifies four novel eosinophilic esophagitis loci. Nat Commun 2014; 5:5593.

23. de Lange KM, Moutsianas L, Lee JC, Lamb CA, Luo Y, Kennedy NA, et al. Genome-wide association study implicates immune activation of multiple integrin genes in inflammatory bowel disease. Nat Genet 2017; 49:256-61.

24. Bonder MJ, Kurilshikov A, Tigchelaar EF, Mujagic Z, Imhann F, Vila AV, et al. The effect of host genetics on the gut microbiome. Nat Genet 2016; 48:1407-12.

25. Tran DQ, Andersson J, Wang R, Ramsey H, Unutmaz D, Shevach EM. GARP (LRRC32) is essential for the surface expression of latent TGF-beta on platelets and activated FOXP3+ regulatory T cells. Proc Natl Acad Sci U S A 2009; 106:13445-50.

26. Manz J, Rodriguez E, ElSharawy A, Oesau EM, Petersen BS, Baurecht H, et al. Targeted Resequencing and Functional Testing Identifies Low-Frequency Missense Variants in the Gene Encoding GARP as Significant Contributors to Atopic Dermatitis Risk. J Invest Dermatol 2016; 136:2380-6.

27. Hughes-Davies L, Huntsman D, Ruas M, Fuks F, Bye J, Chin SF, et al. EMSY links the BRCA2 pathway to sporadic breast and ovarian cancer. Cell 2003; 115:523-35.

28. Ezell SA, Polytarchou C, Hatziapostolou M, Guo A, Sanidas I, Bihani T, et al. The protein kinase Akt1 regulates the interferon response through phosphorylation of the transcriptional repressor EMSY. Proc Natl Acad Sci U S A 2012; 109:E613-21.

29. Purdie KJ, Pourreyron C, South AP. Isolation and culture of squamous cell carcinoma lines. Methods Mol Biol 2011; 731:151-9.

30. Rheinwald JG, Green H. Serial cultivation of strains of human epidermal keratinocytes: the formation of keratinizing colonies from single cells. Cell 1975; 6:331-43.

31. Tanikawa DY, Alonso N, Herson MR, Mathor MB, Caldini EG, Lourenco SV, et al. Ultrastructural evaluation of human keratinocyte growth and differentiation on a fibrin substrate. Acta Cir Bras 2010; 25:541-8.

32. Larcher F, Dellambra E, Rico L, Bondanza S, Murillas R, Cattoglio C, et al. Long-term engraftment of single genetically modified human epidermal holoclones enables safety pre-assessment of cutaneous gene therapy. Mol Ther 2007; 15:1670-6.

33. Meana A, Iglesias J, Del Rio M, Larcher F, Madrigal B, Fresno MF, et al. Large surface of cultured human epithelium obtained on a dermal matrix based on live fibroblast-containing fibrin gels. Burns 1998; 24:621-30.

34. Trynka G. Enhancers looping to target genes. Nat Genet 2017; 49:1564-5.

35. Javierre BM, Burren OS, Wilder SP, Kreuzhuber R, Hill SM, Sewitz S, et al. Lineage-Specific Genome Architecture Links Enhancers and Non-coding Disease Variants to Target Gene Promoters. Cell 2016; 167:1369-84 e19.

36. Rao SS, Huntley MH, Durand NC, Stamenova EK, Bochkov ID, Robinson JT, et al. A 3D map of the human genome at kilobase resolution reveals principles of chromatin looping. Cell 2014; 159:1665-80.

37. Rubin AJ, Barajas BC, Furlan-Magaril M, Lopez-Pajares V, Mumbach MR, Howard I, et al. Lineage-specific dynamic and pre-established enhancer-promoter contacts cooperate in terminal differentiation. Nat Genet 2017; 49:1522-8.

38. Suarez-Farinas M, Tintle SJ, Shemer A, Chiricozzi A, Nograles K, Cardinale I, et al. Nonlesional atopic dermatitis skin is characterized by broad terminal differentiation defects and variable immune abnormalities. J Allergy Clin Immunol 2011; 127:954-64 e1-4.

39. Cole C, Kroboth K, Schurch NJ, Sandilands A, Sherstnev A, O'Regan GM, et al. Filaggrin-stratified transcriptomic analysis of pediatric skin identifies mechanistic pathways in patients with atopic dermatitis. J Allergy Clin Immunol 2014; 134:82-91.

40. Sen GL, Reuter JA, Webster DE, Zhu L, Khavari PA. DNMT1 maintains progenitor function in self-renewing somatic tissue. Nature 2010; 463:563-7.

41. Mildner M, Jin J, Eckhart L, Kezic S, Gruber F, Barresi C, et al. Knockdown of filaggrin impairs diffusion barrier function and increases UV sensitivity in a human skin model. J Invest Dermatol 2010; 130:2286-94.

42. van Smeden J, Janssens M, Kaye EC, Caspers PJ, Lavrijsen AP, Vreeken RJ, et al. The importance of free fatty acid chain length for the skin barrier function in atopic eczema patients. Exp Dermatol 2014; 23:45-52.

43. Okada Y, Wu D, Trynka G, Raj T, Terao C, Ikari K, et al. Genetics of rheumatoid arthritis contributes to biology and drug discovery. Nature 2014; 506:376-81.

44. Sullivan PF, Agrawal A, Bulik CM, Andreassen OA, Borglum AD, Breen G, et al. Psychiatric Genomics: An Update and an Agenda. Am J Psychiatry 2018; 175:15-27.

45. Sud A, Kinnersley B, Houlston RS. Genome-wide association studies of cancer: current insights and future perspectives. Nat Rev Cancer 2017; 17:692-704.

46. Bulger M, Groudine M. Functional and mechanistic diversity of distal transcription enhancers. Cell 2011; 144:327-39.

47. Pennisi E. Genomics. ENCODE project writes eulogy for junk DNA. Science 2012; 337:1159, 61.

48. Potaczek DP, Harb H, Michel S, Alhamwe BA, Renz H, Tost J. Epigenetics and allergy: from basic mechanisms to clinical applications. Epigenomics 2017; 9:539-71.

49. Palmer CN, Irvine AD, Terron-Kwiatkowski A, Zhao Y, Liao H, Lee SP, et al. Common loss-of-function variants of the epidermal barrier protein filaggrin are a major predisposing factor for atopic dermatitis. Nat Genet 2006; 38:441-6.

50. Lee UH, Kim BE, Kim DJ, Cho YG, Ye YM, Leung DY. Atopic dermatitis is associated with reduced corneodesmosin expression: role of cytokine modulation and effects on viral penetration. Br J Dermatol 2017; 176:537-40.

51. Totsuka A, Omori-Miyake M, Kawashima M, Yagi J, Tsunemi Y. Expression of keratin 1, keratin 10, desmoglein 1 and desmocollin 1 in the epidermis: possible downregulation by interleukin-4 and interleukin-13 in atopic dermatitis. Eur J Dermatol 2017; 27:247-53.

52. Gruber F, Kremslehner C, Narzt MS. The impact of recent advances in lipidomics and redox lipidomics on dermatological research. Free Radic Biol Med 2019.

53. O'Regan GM, Campbell LE, Cordell HJ, Irvine AD, McLean WH, Brown SJ. Chromosome 11q13.5 variant associated with childhood eczema: an effect supplementary to filaggrin mutations. J Allergy Clin Immunol 2010; 125:170-4 e1-2.

54. Paternoster L, Savenije OEM, Heron J, Evans DM, Vonk JM, Brunekreef B, et al. Identification of atopic dermatitis subgroups in children from 2 longitudinal birth cohorts. J Allergy Clin Immunol 2018; 141:964-71.

55. ExAC. Exome Aggregation Consortium http://exac.broadinstitute.org/gene/ENSG00000158636. 2018.

56. EVS. Exome Variant Server http://evs.gs.washington.edu/EVS/. 2018.

57. gnomAD. Genome Aggregation Database http://gnomad.broadinstitute.org/gene/ENSG00000158636. 2018.

58. Maurano MT, Humbert R, Rynes E, Thurman RE, Haugen E, Wang H, et al. Systematic localization of common disease-associated variation in regulatory DNA. Science 2012; 337:1190-5.

59. Patil VS, Madrigal A, Schmiedel BJ, Clarke J, O'Rourke P, de Silva AD, et al. Precursors of human CD4(+) cytotoxic T lymphocytes identified by single-cell transcriptome analysis. Sci Immunol 2018; 3.

60. Davies JO, Telenius JM, McGowan SJ, Roberts NA, Taylor S, Higgs DR, et al. Multiplexed analysis of chromosome conformation at vastly improved sensitivity. Nat Methods 2016; 13:74-80.

61. Franke L, Jansen RC. eQTL analysis in humans. Methods Mol Biol 2009; 573:311-28.

62. Liu B, Gloudemans MJ, Rao AS, Ingelsson E, Montgomery SB. Abundant associations with gene expression complicate GWAS follow-up. Nat Genet 2019; 51:768-9.

63. Kretz M, Siprashvili Z, Chu C, Webster DE, Zehnder A, Qu K, et al. Control of somatic tissue differentiation by the long non-coding RNA TINCR. Nature 2013; 493:231-5.

64. Cevikbas F, Wang X, Akiyama T, Kempkes C, Savinko T, Antal A, et al. A sensory neuron-expressed IL-31 receptor mediates T helper cell-dependent itch: Involvement of TRPV1 and TRPA1. J Allergy Clin Immunol 2014; 133:448-60.

65. Hendricks AJ, Vaughn AR, Clark AK, Yosipovitch G, Shi VY. Sweat mechanisms and dysfunctions in atopic dermatitis. J Dermatol Sci 2018; 89:105-11.

66. Raguz J, Jeric I, Niault T, Nowacka JD, Kuzet SE, Rupp C, et al. Epidermal RAF prevents allergic skin disease. Elife 2016; 5.

67. Blunder S, Ruhl R, Moosbrugger-Martinz V, Krimmel C, Geisler A, Zhu H, et al. Alterations in Epidermal Eicosanoid Metabolism Contribute to Inflammation and Impaired Late Differentiation in FLG-Mutated Atopic Dermatitis. J Invest Dermatol 2017; 137:706-15.

68. Simpson EL, Bruin-Weller M, Flohr C, Ardern-Jones MR, Barbarot S, Deleuran M, et al. When does atopic dermatitis warrant systemic therapy? Recommendations from an expert panel of the International Eczema Council. J Am Acad Dermatol 2017; 77:623-33.

69. Jobard F, Lefevre C, Karaduman A, Blanchet-Bardon C, Emre S, Weissenbach J, et al. Lipoxygenase-3 (ALOXE3) and 12(R)-lipoxygenase (ALOX12B) are mutated in non-bullous congenital ichthyosiform erythroderma (NCIE) linked to chromosome 17p13.1. Hum Mol Genet 2002; 11:107-13.

70. Smith FJ, Irvine AD, Terron-Kwiatkowski A, Sandilands A, Campbell LE, Zhao Y, et al. Loss-of-function mutations in the gene encoding filaggrin cause ichthyosis vulgaris. Nat Genet 2006; 38:337-42.

71. Smith FJ, Maingi C, Covello SP, Higgins C, Schmidt M, Lane EB, et al. Genomic organization and fine mapping of the keratin 2e gene (KRT2E): K2e V1 domain polymorphism and novel mutations in ichthyosis bullosa of Siemens. J Invest Dermatol 1998; 111:817-21.

72. Wirth B, Herrmann FH, Neugebauer M, Gillard EF, Wulff K, Stein C, et al. Linkage analysis in X-linked ichthyosis (steroid sulfatase deficiency). Hum Genet 1988; 80:191-2.

73. Kogame T, Dainichi T, Shimomura Y, Tanioka M, Kabashima K, Miyachi Y. Palmoplantar keratosis in oculodentodigital dysplasia with a GJA1 point mutation out of the C-terminal region of connexin 43. J Dermatol 2014; 41:1095-7.

74. Oji V, Eckl KM, Aufenvenne K, Natebus M, Tarinski T, Ackermann K, et al. Loss of corneodesmosin leads to severe skin barrier defect, pruritus, and atopy: unraveling the peeling skin disease. Am J Hum Genet 2010; 87:274-81.

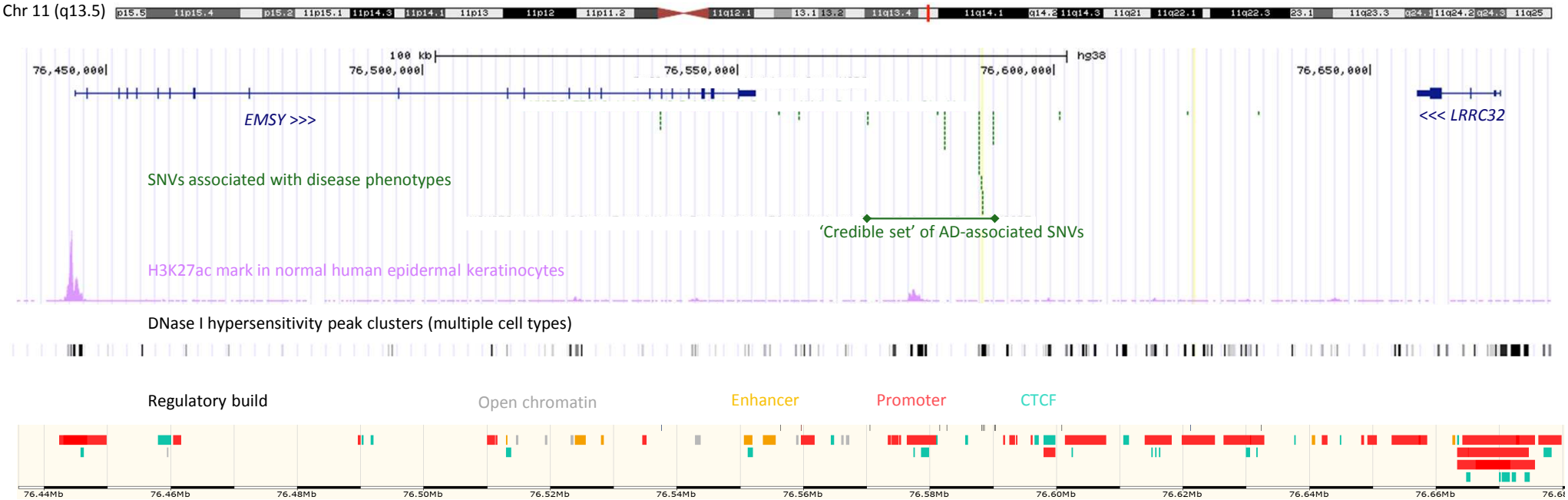
ACCEPTED MANUSCRIPT

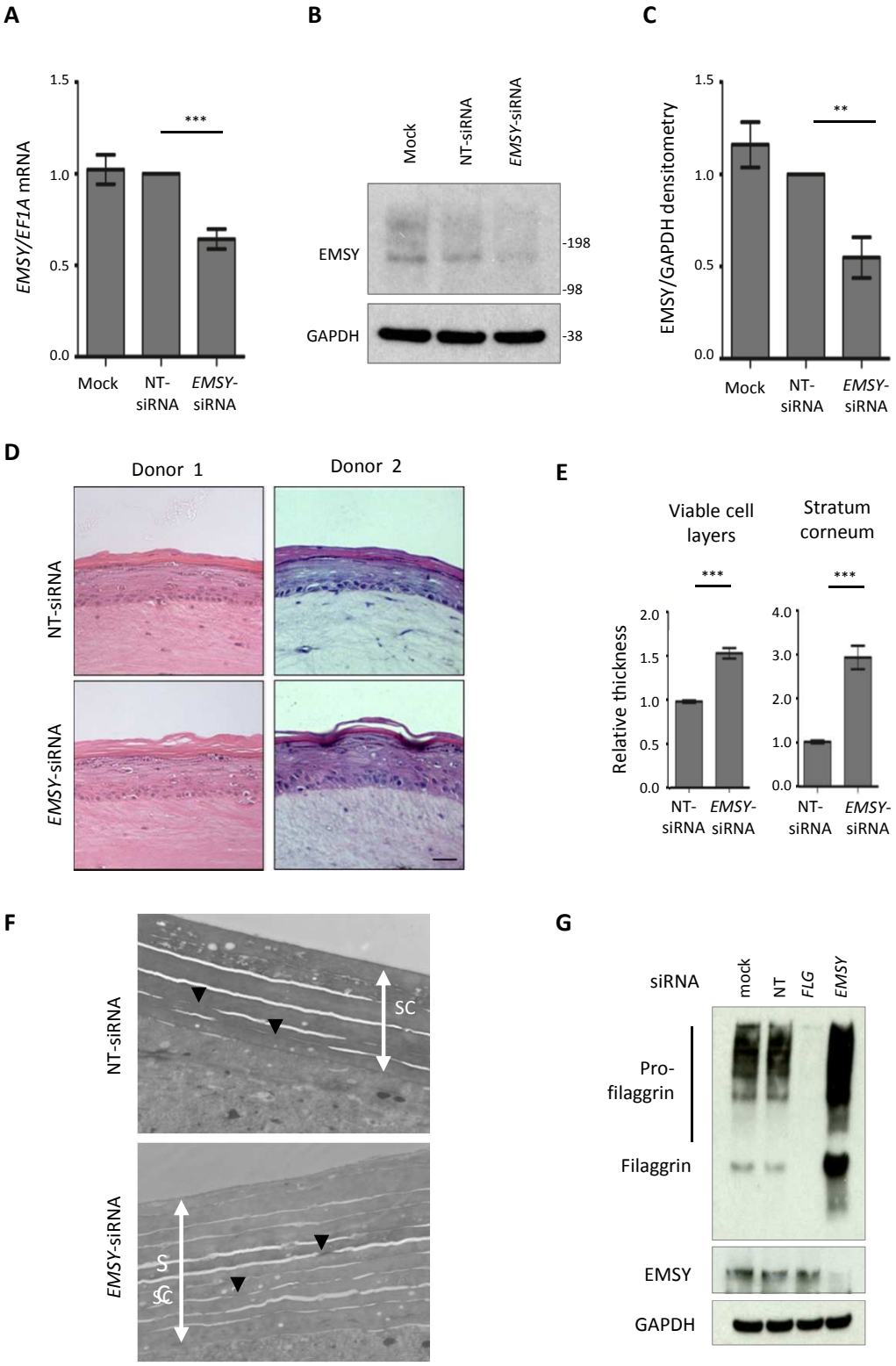
754 75. Christiano AM, Greenspan DS, Hoffman GG, Zhang X, Tamai Y, Lin AN, et al. A missense
755 mutation in type VII collagen in two affected siblings with recessive dystrophic epidermolysis
756 bullosa. Nat Genet 1993; 4:62-6.
757

758

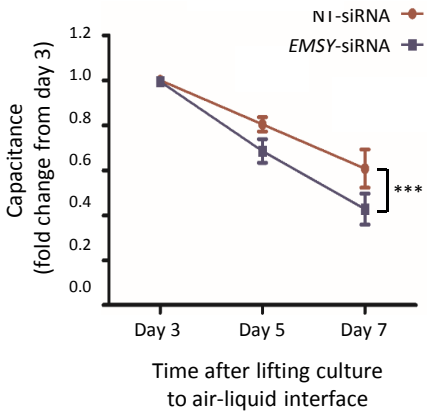
ACCEPTED MANUSCRIPT

UCSC Genome Browser Human and Ensembl (GRCh38/hg38)

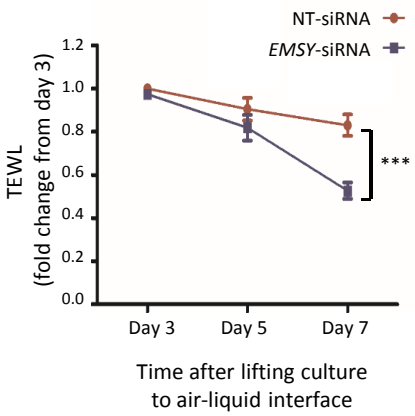



A
B
C
D
E
F
G
EMSY/EF1A mRNA
1.5
1.0
0.5
0.0
***
Mock
NT-siRNA
EMSY-siRNA
Mock
NT-siRNA
EMSY-siRNA
EMSY
GAPDH
-198
-98
-38
EMSY/GAPDH densitometry
**
Donor 1
Donor 2
NT-siRNA
EMSY-siRNA
Viable cell layers
Stratum corneum
Relative thickness
2.0
1.5
1.0
0.5
0.0
4.0
3.0
2.0
1.0
SC
siRNA
mock
NT
FLG
EMSY
Pro-filaggrin
Filaggrin
EMSY
GAPDH

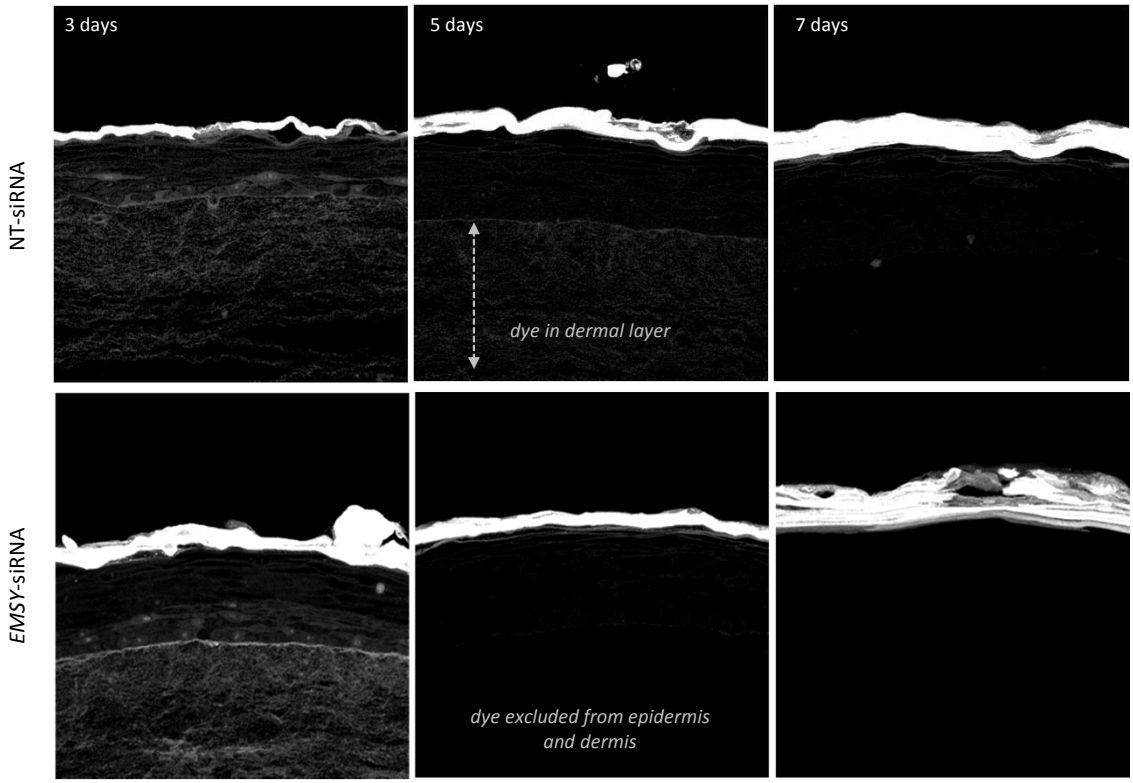
A


NT-siRNA
EMSY-siRNA
Capacitance
(fold change from day 3)
1.2
1.0
0.8
0.6
0.4
0.2
0.0
***
Day 3
Day 5
Day 7
Time after lifting culture
to air-liquid interface

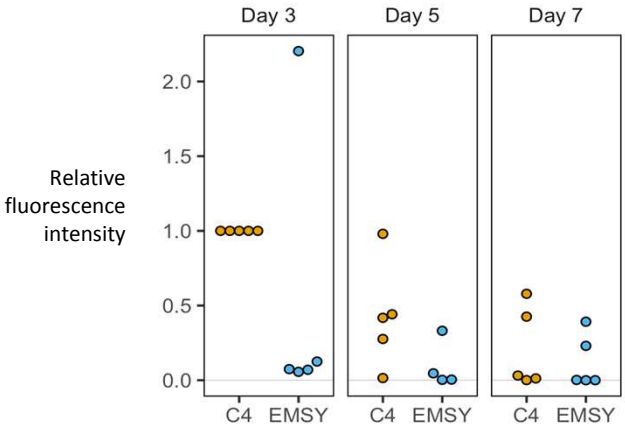
B

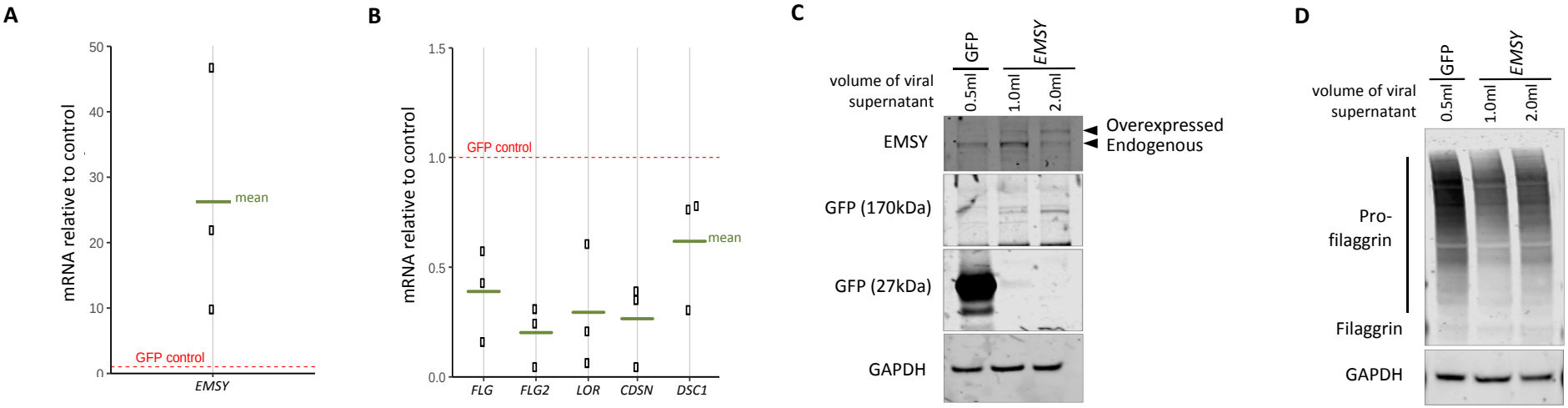

NT-siRNA
EMSY-siRNA
TEWL
(fold change from day 3)
1.2
1.0
0.8
0.6
0.4
0.2
0.0
***
Day 3
Day 5
Day 7
Time after lifting culture
to air-liquid interface

C

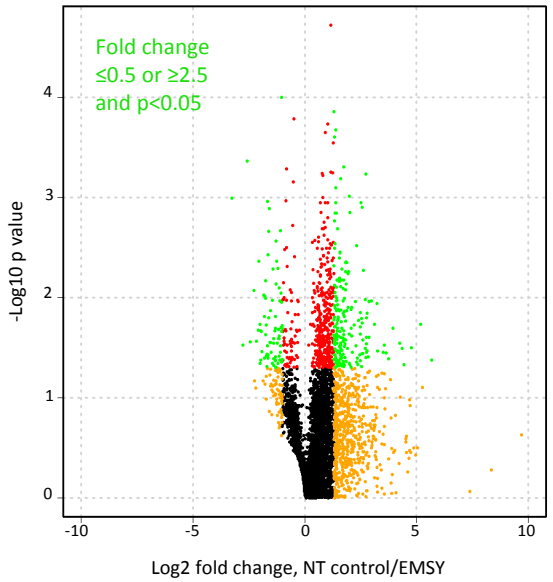

3 days
5 days
7 days
NT-siRNA
dye in dermal layer
EMSY-siRNA
dye excluded from epidermis
and dermis

D

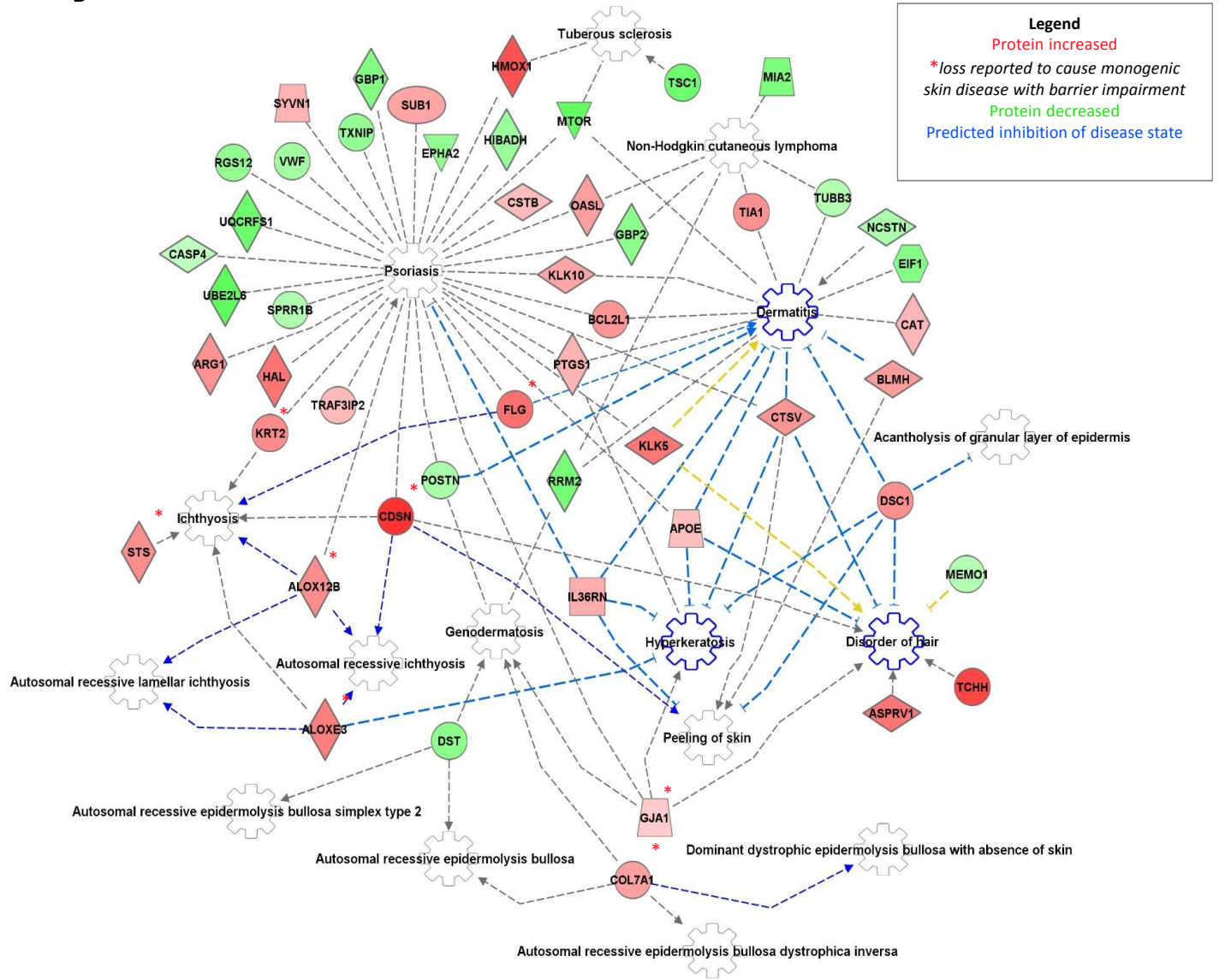

Day 3
Day 5
Day 7
Relative
fluorescence
intensity
2.0
1.5
1.0
0.5
0.0
C4
EMSY
C4
EMSY
C4
EMSY

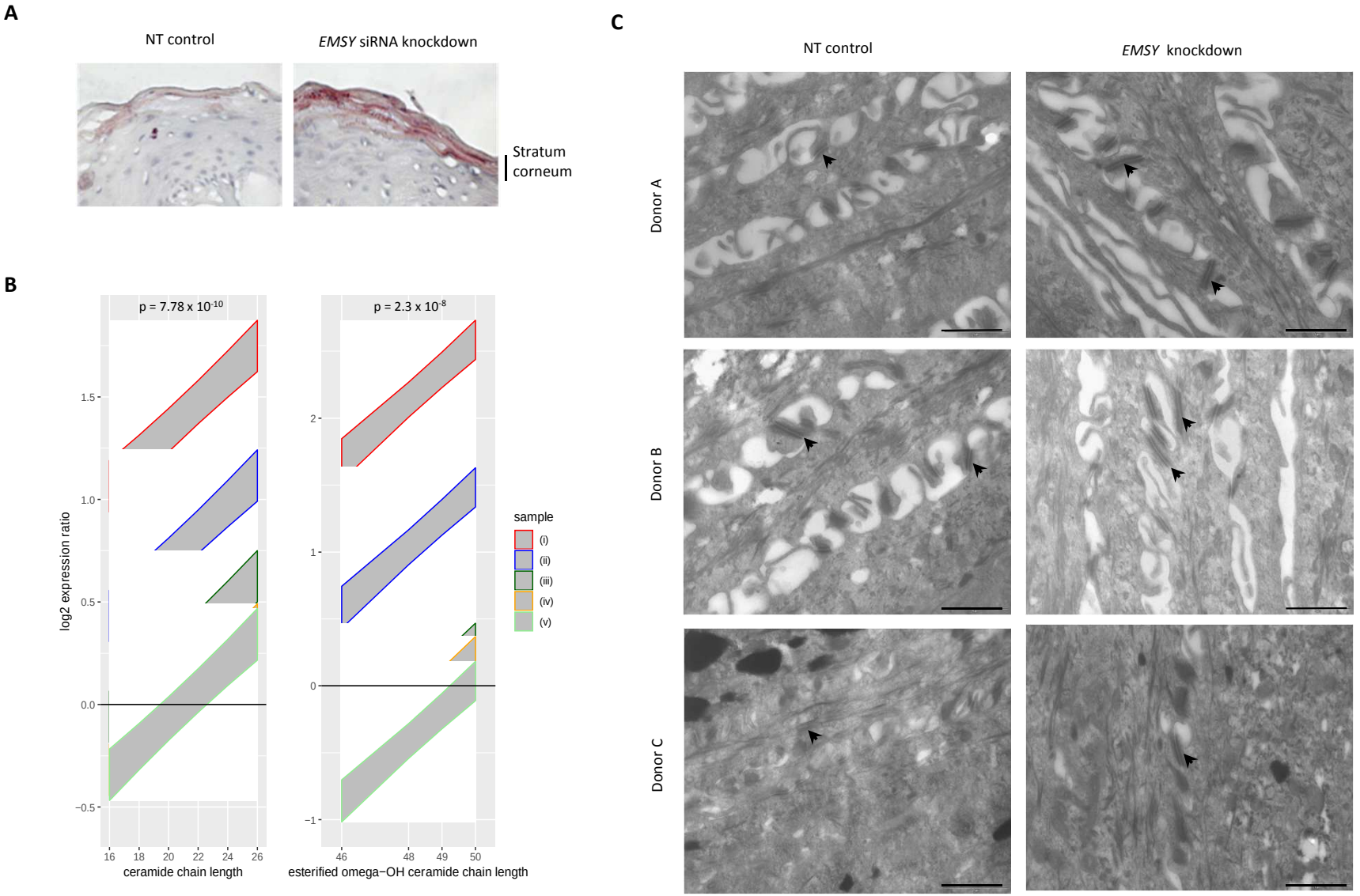

A
mRNA relative to control
50
40
30
20
10
0
mean
GFP control
EMSY
B
mRNA relative to control
1.5
1.0
0.5
0.0
GFP control
mean
FLG
FLG2
LOR
CDSN
DSC1
C
volume of viral supernatant
GFP
EMSY
0.5ml
1.0ml
2.0ml
EMSY
Overexpressed
Endogenous
GFP (170kDa)
GFP (27kDa)
GAPDH
D
volume of viral supernatant
GFP
EMSY
0.5ml
1.0ml
2.0ml
Pro-filaggrin
Filaggrin
GAPDH

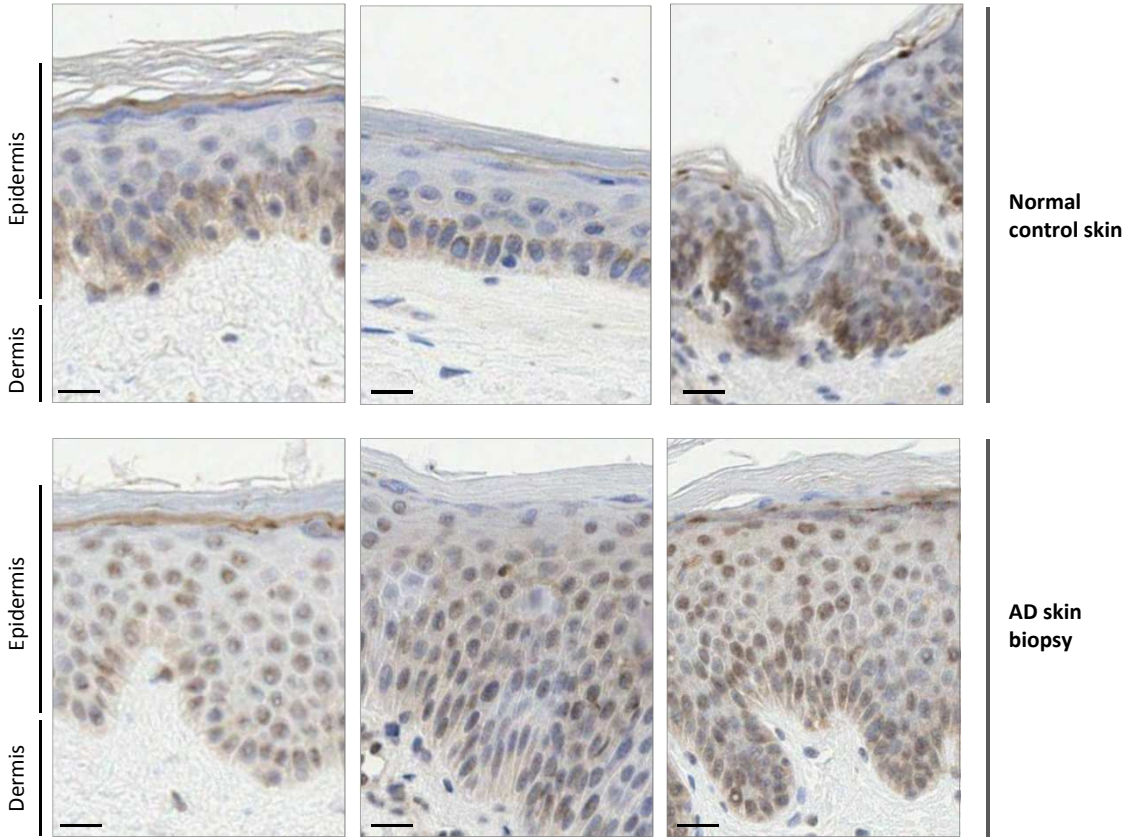
A


Fold change
≤0.5 or ≥2.5
and p<0.05
-Log10 p value
Log2 fold change, NT control/EMSY
4
3
2
1
0
-10
-5
0
5
10

B


Legend
Protein increased
*loss reported to cause monogenic skin disease with barrier impairment
Protein decreased
Predicted inhibition of disease state
Tuberous sclerosis
HMOX1
TSC1
MIA2
GBP1
SUB1
SYVN1
TXNIP
EPHA2
HIBADH
MTOR
Non-Hodgkin cutaneous lymphoma
RGS12
VWF
CSTB
OASL
TIA1
TUBB3
NCSTN
UQCRFS1
GBP2
CASP4
Psoriasis
KLK10
EIF1
UBE2L6
SPRR1B
BCL2L1
Dermatitis
CAT
ARG1
HAL
PTGS1
BLMH
TRAF3IP2
FLG
CTSV
KRT2
KLK5
Acantholysis of granular layer of epidermis
POSTN
RRM2
DSC1
Ichthyosis
CDSN
APOE
STS
MEMO1
ALOX12B
IL36RN
Genodermatosis
Hyperkeratosis
Disorder of hair
Autosomal recessive ichthyosis
Autosomal recessive lamellar ichthyosis
TCHH
ASPRV1
ALOXE3
DST
Peeling of skin
GJA1
Autosomal recessive epidermolysis bullosa simplex type 2
Dominant dystrophic epidermolysis bullosa with absence of skin
Autosomal recessive epidermolysis bullosa
COL7A1
Autosomal recessive epidermolysis bullosa dystrophica inversa


A
NT control
EMSY siRNA knockdown
Stratum corneum
B
p = 7.78 x 10-10
p = 2.3 x 10-8
log2 expression ratio
ceramide chain length
esterified omega−OH ceramide chain length
sample
(i)
(ii)
(iii)
(iv)
(v)
C
NT control
EMSY knockdown
Donor A
Donor B
Donor C


Epidermis
Dermis
Normal
control skin
Epidermis
Dermis
AD skin
biopsy

ACCEPTED MANUSCRIPT

SUPPLEMENTARY METHODS

Promoter-capture Hi-C data analysis

Fastq files from Rubin *et al*.[1] were processed with the HiCUP pipeline version 0.6.1 (https://www.bioinformatics.babraham.ac.uk/projects/hicup/) which truncated, mapped, filtered and de-duplicated reads. Reference genome GRCh37 was used for mapping. Loci containing five AD-associated SNVs from the GWAS catalogue were investigated (rs11236809, rs7927894, rs2155219, rs2212434 and rs7130588) and genes within 250kb. Six baits within regions of 100kb around each SNP and genes of interest were identified. Bait-region interaction plots were generated for each of the baits using BioConductor package CHiCAGO[2] version 1.10.1

RT-qPCR

RNA was extracted from organotypic epidermis using the Direct-zol RNA kit (Zymo Research, Irvine, California, USA) following homogenisation in RNA Bee (Amsbio, Abingdon,Oxfordhire, UK) using the TissueLyser LT (Qiagen, Manchester, UK) 5 mins at 50 Hz. cDNA was prepared from 1µg total RNA using random priming (2.5µM final) (Integrated DNA Technologies, Coralville, Iowa, USA) in combination with Moloney murine leukemia virus enzyme (MMLV) (100 units) and buffer systems (Life Technologies, Carlsbad, California, USA). qPCR reactions were performed using exon spanning probe-based assays (**Table E1,** below) in combination with TaqMan gene expression Mastermix (Life Technologies, Carlsbad, California, USA). Reactions were prepared and run using the Qiagility robot in combination with the Rotorgene Q (Qiagen, Manchester, UK). *EF1A* was used as a reference gene and fold changes were derived via the 2(-Delta Delta C(T)) method.

Immunoblotting

Organotypic epidermis was homogenized in RIPA buffer (Cell Signalling Technologies, London, UK) using the TissueLyser LT (Qiagen, Manchester, UK) 5 mins at 50 Hz. Protein lysates were normalized by Pierce BCA assay (Thermo Fisher, Waltham, Massachussets, USA) and resolved under reducing conditions using the NuPage® gel electrophoresis system (Life Technologies, Carlsbad, California, USA). Primary antibodies were prepared in 5% bovine serum albumin (BSA) and incubated overnight at 4^{o}C with agitation (**Table E2,** below). Immunoblots were developed using peroxidase conjugated secondary antibodies (DAKO, Glostrup, Denmark, 1:5000) in combination with Chemiluminescent HPR substrate (Immobilon, Millipore, Billerica, Massachussets, USA) onto photographic film. Densitometry was performed using ImageJ.

Image analysis for measurement of epidermal thickness

Histological sections of 10 replicate skin organotypic experiments were measured using a standardized technique to minimize bias, as follows: Three points were measured on each slide, at

the right side, middle and left of each sample, across viable cell layers and stratum corneum; measurements were generated using ImageJ and the mean of the three measurements calculated.

Immunohistochemistry and immunofluorescence

Formalin-fixed, paraffin embedded normal skin and AD samples were processed in unison for immunohistochemistry. Staining was performed using the automated EnVision+ system in combination with DAB detection and haematoxylin counterstain (DAKO, Tayside Tissue Bank service). Slides were imaged using the automated Aperio ImageScope slide scanner allowing deep zoom magnification (Leica Biosystems, Wetzlar, Germany Biosystems). Formalin-fixed, paraffin embedded full thickness organotypics were processed by immunofluorescence under standard conditions using an Alexa Fluor 568 conjugated secondary antibody and DAPI counterstain (Life Technologies, Carlsbad, California, USA). Negative control sections were stained in the absence of a primary antibody. Slides were imaged by confocal Zeiss LSM710 microscope (Carl Zeiss Microscopy GmbH, Jena, Germany). Antibodies are detailed in **Table E3** (below).

Transmission electron microscopy

Organotypic skin samples were fixed in 4% paraformaldehyde, 2.5% gluteraldehyde in 0.1M sodium cacodylate buffer (pH 7.2) for one hour then cut into small pieces, washed in buffer and post-fixed in 1% osmium tetroxide in cacodylate buffer for one hour. The pieces were dehydrated through alcohol series, into propylene oxide and embedded in Durcupan resin. Ultrathin sections were stained with 3% aqueous uranyl acetate and Reynold's lead citrate and examined on a JEOL 1200EX electron microscope. Images were collected on a SIS Megaview III camera.

Mass spectrometry proteomic analysis

Frozen organotypic epidermal samples were ground on dry ice, solubilized in 200µl of Cellular and Organelle Membrane Solubilizing Reagent (Sigma-Aldrich, Gillingham, Dorset, UK), 7.0 M urea, 2.0 M thiourea, 40 mM Trizma® base (Sigma Aldrich, Gillingham, Dorset, UK) and 1.0% C7BzO, pH 10.4 buffer with protease inhibitors. The lysate was acetone precipitated for 1 hour at -20^{o}C and spun for 20 mins at 2^{o}C at 15,000 rpm. The pellet was re-suspended in 200µl of 50mM ammonium bicarbonate. 100µl was taken for in-solution digest. 22µl of dithiothreitol was added and samples heated to 50^{o}C for 15mins. 24µl of iodoacetamide was added and the samples incubated at 22^{o}C for 30 mins. 1µl of Rapigest was added, followed by 2.5µl of trypsin, for a 12-hour digest. A further 1µl trypsin was added for an additional 4-hour digest. The peptide samples were fractionated into 24 fractions with high pH Reversed Phase C18 chromatography, run on a Q Exactive Classic or Plus for 160 mins and the top 15 ions selected for sequencing. MS resolution was 70,000 and MS/MS resolution 17,500. Data were processed using MaxQuant (v1.6.0.13) and Human UniProt Database (Dec 2017) with a protein and peptide false discovery rate of 0.01.

Proteins identified as contaminants (trypsin and other lab originating proteins) and contained within the MaxQuant database (http://www.maxquant.org/maxquant/) were removed. To account for the possibility of keratin as a contaminant, we analysed the blank runs for keratin peptide intensity and subtracted this from the measured keratin intensities. A reversed database (i.e. scrambled protein sequences) was used to identify false positives and these were also removed. Total intensities of the samples were normalized to total protein abundance, with adjustment to the lowest total protein yield. All samples were run in quadruplicate to test reproducibility; the Pearson correlations were 0.86-0.92 (**Fig. E6**).

Mass spectrometry lipidomic analysis

Skin samples were sonicated in phosphate buffered saline (pH7.4) and then extracted according to the method of Folch *et al.*[3]. Ceramide 17:0 (Avanti Polar Lipids, Alabaster, AL, USA) was included in the experimental system as an internal standard. The skin lipids were analysed by liquid chromatography-mass spectrometry (LC-MS) on a Thermo Exactive Orbitrap mass spectrometer (Thermo Scientific, Hemel Hempsted, UK) coupled to a Thermo Accela 1250 ultra high pressure liquid chromatography (UHPLC) system. Samples were injected on to C18 column (Thermo Hypersil Gold, 2.1 mm x 100 mm, 1.9 µm) and separated using a water/acetonitrile/isopropanol gradient[4]. Ion signals corresponding to individual ceramide molecular species were extracted from raw LC-MS data sets. The concentration of each ceramide was expressed as pmol/mg after normalisation to mg of wet weight tissue. Chain lengths reported in our data correspond to ceramides reported in AD skin *in vivo* as follows: Cer22 relates to NS CER 40 carbons in work by van Smeden *et al* [5] and esterified omega-hydroxy ceramide d18:1/50:2 species are equivalent of acyl-CER with 68 carbons, each of which show reduced abundance in AD skin *in vivo*[5].

Lipid data analysis

Ceramide and esterified omega-hydroxy-ceramide data were analysed separately and matched samples were compared using replicate experimental data without pooling. The ratio of lipid concentration was computed, to compare *EMSY* siRNA-treated organotypic with donor-matched control sample; results were log transformed using natural log ($\log_e$). To investigate a trend in differential expression dependent on lipid length, a linear model was fitted and plotted with 95% confidence intervals; p-values were computed for the term in the linear model for chain length, where $p<0.05$ indicates a significant difference in lipid length between *EMSY* siRNA-treated samples and controls. Analyses were performed with R-style formula "<logged-expression-ratio> ~ <lipid-length> + <sample>" and the glm function in R (version 3.5.1); data and the linear models were plotted with the R package ggplot2 (version 3.1.0).

ACCEPTED MANUSCRIPT

Clinical samples used for immunohistochemistry

Control skin was obtained from adult patients, with written informed consent, as surplus tissue generated from routine surgical procedures. Male and female patients, with clinically normal skin were used. Individuals having undergone systemic chemotherapy were excluded.

AD skin samples were obtained as surplus to clinical care and used with written informed consent. Demographic and phenotypic features of these patients are shown in **Table E4** (below). Samples were identified from the pathology database by searching for the histological diagnosis of eczema or dermatitis, with spongiosis; samples with any features of other forms of dermatitis (eg stasis changes, marked eosinophilic infiltration, photodamage or signs of external trauma) were not selected for the study. There was no apparent correlation between skin site, gender, age or AD severity and EMSY immunostaining.

ACCEPTED MANUSCRIPT

ACCEPTED MANUSCRIPT

GENE NAME	ASSAY ID/SEQUENCE	CONCENTRATION
FLG	HS.PT.58.24292320 (FAM/ZEN/IBFQ) (Integrated DNA Technologies)	PRIMERS: 500 NM PROBE: 250 NM
EMSY	Hs.PT.58.28326190 (FAM/ZEN/IBFQ) (Integrated DNA Technologies)	PRIMERS: 500 NM PROBE: 250 NM
EF1A	Hs.PT.58.24345862 (FAM/ZEN/IBFQ) (Integrated DNA Technologies)	PRIMERS: 500 NM PROBE: 250 NM
CDSN	F: ATGATGGCACTGCTGCTG R: AAGGTGCCAATGCTCTTAGC P: UPL#51	PRIMERS: 400 NM PROBE: 100 NM
DSC1	F: GGGGCAGGGAGATACTGG R: CAGAGTGTGTCCTCTAATGGATTC P: UPL#53	PRIMERS: 400 NM PROBE: 100 NM
FLG2	F: CTGACTATGGCCTGCAACAA R: CTTTGACCCTGAAGCTTTGC P: UPL#73	PRIMERS: 400 NM PROBE: 100 NM
K2	F: GCCTCCTTCATTGACAAGGT R: GCTGTCGATATACCCCTGGA P: UPL#1	PRIMERS: 400 NM PROBE: 100 NM
HAL	F: GAACTGAACAGCGCAACAGA R: TTTGGCTGGGTATTCACCAT P: UPL#65	PRIMERS: 400 NM PROBE: 100 NM
BLMH	F: AGGGAACATGTCAAGCCACT R: TTCCACTGTGTAAAGTTTGTTGTACTT P: UPL#57	PRIMERS: 400 NM PROBE: 100 NM
ASPRV1	F: TCTGTGGTCCACCCAAACTT R: GCTGCAGGGTGTCCAGAT P: UPL#52	PRIMERS: 400 NM PROBE: 100 NM
ALOXE3	F: CAAGAACCCAAGGACCAGAG R: TCCTGGATGTCCCTTGAGAT P: UPL#82	PRIMERS: 400 NM PROBE: 100 NM
ALOX12B	F: GCTACGAGACCCTGGCACT R: AGAAGTCCTGCTTGGCTCTG P: UPL#1	PRIMERS: 400 NM PROBE: 100 NM
STS	F: CATGGACATATTTCCTACAGTAGCC R: CACGTCCATCAATGATCCTGT P: UPL#19	PRIMERS: 400 NM PROBE: 100 NM
APOE	F: CAGGCAGGAAGATGAAGGTT R: CTGTCTCCACCGCTTGCT P: UPL#72	PRIMERS: 400 NM PROBE: 100 NM
COL7A1	F: GCTGGTGCTGCCTTTCTCT R: TCCAGGCCGAACTCTGTC P: UPL#71	PRIMERS: 400 NM PROBE: 100 NM
MTOR	F: TTTAGCGGTCATGTCAATGG R: CATCAGGTTGGATGGGTGT P: UPL#14	PRIMERS: 400 NM PROBE: 100 NM
IL36RN	F: GCAGGGAAGGTCATTAAAGGT R: CCTGGACACCCAGGATGA P: UPL#42	PRIMERS: 400 NM PROBE: 100 NM
CDK1	F:TGGATCTGAAGAAATACTTGGATTCTA R:TCTGGAGATCTGTACCAGAGTGTT P: UPL#79	PRIMERS: 400 NM PROBE: 100 NM
RNASE7	F:GAAGACCAAGCGCAAAGC R:AGCAGAAGGGGGCAGAAT P: UPL#63	PRIMERS: 400 NM PROBE: 100 NM
GJA1	F:GCCTGAACTTGCCTTTTCAT R: CTCCAGTCACCCATGTTGC P: UPL#88	PRIMERS: 400 NM PROBE: 100 NM

Table E1. qPCR assay details

F: forward primer, R: reverse primer, P: probe, UPL: Universal Probe Library and corresponding probe number (#) (Sigma Aldrich).

PROTEIN NAME	MANUFACTURER / CLONE	1° ANTIBODY DILUTION
FILAGGRIN	Santa Cruz sc66192	1/250
EMSY	Bethyl Laboratories A300-253A	1/2000
KERATIN, TYPE II CYTOSKELETAL 2 EPIDERMAL	Abcam ab170106	1/1000
HISTADINE AMMONIA-LYASE	Thermo Fisher PA1-518	1/800
SERINE/THREONINE-PROTEIN KINASE MTOR	Thermo Fisher PA1-518	1/500
ARACHIDONATE 12-LIPOXYGENASE	Thermo Fisher PS5-23608	1/1000
CORNEODESMOSIN	Thermo Fisher PA5-47768	1/200
DESMOCOLLIN-1	Novus NBP-1-88099	1/1000
FILAGGRIN-2	Abcam ab122011	1/500
STERYL-SULFATASE	Abcam ab62219	1/1000
HYDROPEROXIDE ISOMERASE ALOXE	Thermo Fisher PA5-2183	1/3000
GAP JUNCTION ALPHA-1 PROTEIN	Thermo Fisher 71-0700	1/500
INTERLEUKIN-36 RECEPTOR ANTAGONIST	ATLAS HPA034542	1/200
GYLYCERALDEHYDE-3-PHOSPHATE DEHYDROGENASE	Cell signalling 97166	1/10,000

Table E2. Immunoblotting antibody details

PROTEIN NAME	MANUFACTURER / CLONE	1° ANTIBODY DILUTION	HIER
FILAGGRIN	Santa Cruz sc66192	1/1000	TRIS/EDTA
EMSY	Bethyl Laboratories A300-253A	1/250	Tris/EDTA
KERATIN, TYPE II CYTOSKELETAL 2 EPIDERMAL	Thermo Fisher PA5-21456	1/500	CITRATE
HISTADINE AMMONIA-LYASE	ATLAS HPA038547	1/500	CITRATE
SERINE/THREONINE-PROTEIN KINASE MTOR	Thermo Fisher PA1-518	1/200	CITRATE
ARACHIDONATE 12-LIPOXYGENASE	Thermo Fisher PS5-23608	1/200	CITRATE
CORNEODESMOSIN	Thermo Fisher PA5-47768	1/200	CITRATE
DESMOCOLLIN-1	Novus NBP-1-88099	1/200	CITRATE

Table E3. Immunohistochemistry and immunofluorescence antibody details

HIER: heat induced epitope retrieval method

ACCEPTED MANUSCRIPT

Age (years)	Sex	Site of biopsy	Clinical features	Histological diagnosis
28	Female	right abdominal skin	itchy lesion	subacute dermatitis
66	Female	areolar	severe eczema	dermatitis, eczematous
50	Female	areolar	eczema	very occasional eosinophils
23	Female	areolar	eczema	dermatitis, eczematous
29	Female	areolar	mild eczema	dermatitis, eczematous
60	Female	skin overlying left hip	atopic eczema and widespread flare	spongiotic dermatitis
49	Male	right neck	atopic background	area of chronic dermatitis
49	Female	right cheek	itchy lesion	mild spongiosis, chronic dermatitis
64	Female	areolar	moderately severe eczema	dermatitis, eczematous
19	Female	right inner upper arm	patchy dry rash	mild chronic dermatitis
62	Male	mid-back	itchy	mild spongiosis, mild chronic dermatitis
48	Female	right medial wrist	atopic eczema	chronic spongiotic dermatitis
55	Male	left forearm	erythroderma	mild spongiosis, subacute dermatitis
24	Female	right flank	atopic dermatitis flare	chronic spongiotic dermatitis

Table E4. Demographic and phenotypic features of patients from whom skin biopsy samples were obtained.

ACCEPTED MANUSCRIPT

ACCEPTED MANUSCRIPT

References

1. Rubin AJ, Barajas BC, Furlan-Magaril M, Lopez-Pajares V, Mumbach MR, Howard I, et al. Lineage-specific dynamic and pre-established enhancer-promoter contacts cooperate in terminal differentiation. Nat Genet 2017; 49:1522-8.
2. Cairns J, Freire-Pritchett P, Wingett SW, Varnai C, Dimond A, Plagnol V, et al. CHiCAGO: robust detection of DNA looping interactions in Capture Hi-C data. Genome Biol 2016; 17:127.
3. Folch J, Lees M, Sloane Stanley GH. A simple method for the isolation and purification of total lipides from animal tissues. J Biol Chem 1957; 226:497-509.
4. McIlroy GD, Tammireddy SR, Maskrey BH, Grant L, Doherty MK, Watson DG, et al. Fenretinide mediated retinoic acid receptor signalling and inhibition of ceramide biosynthesis regulates adipogenesis, lipid accumulation, mitochondrial function and nutrient stress signalling in adipocytes and adipose tissue. Biochem Pharmacol 2016; 100:86-97.
5. van Smeden J, Janssens M, Kaye EC, Caspers PJ, Lavrijsen AP, Vreeken RJ, et al. The importance of free fatty acid chain length for the skin barrier function in atopic eczema patients. Exp Dermatol 2014; 23:45-52.

ACCEPTED MANUSCRIPT

Supplementary Figure Legends

Figure E1. Chromosomal conformation data analysis

a. Data from Rao *et al.* (2014) generated using normal human keratinocytes, displayed in the Hi-C data browser from Yue lab, Penn State, USA http://promoter.bx.psu.edu/hi-c/view.php?method=Hi-C&species=human&assembly=hg19&source=inside&tissue=NHEK&type=Liebermanraw&resolution=5&c_url=&transfer=&gene=&chr=chr11&start=75553333.333333&end=76871666.666667&sessionID=&browser=none

b. Data from Rubin *et al.* (2017) generated using normal human keratinocytes in duplicate experiments. Results are shown for day 0; cells differentiated to days 3 and 6 gave very similar results. Coloured rectangles indicate position of the genes and blue lines show the SNP positions. The vertical red line is the location of the bait. Plots shows read count added across the two replicate experiments. There is some evidence of an interaction between the SNP region and *LRRC32*, but an interaction with *EMSY* cannot be excluded.

Figure E2. Direct (single molecule) RNA sequencing of atopic skin compared to non-atopic control skin

Direct RNA sequencing analysis (48) of skin biopsies from the clinically uninflamed skin of paediatric AD patients (n=26) and site-matched non-atopic control skin (n=10); box plots show median, first and third quartiles, whiskers extend to most extreme data point <1.5 x interquartile range; p>0.05

Details of the donor phenotypes and demographic details are reported in Cole *et al.* (2014).

Figure E3. Comparison of effects of individual and pooled EMSY-siRNAs

a. Bar chart showing mean EMSY mRNA; error bars show standard deviaEon; C4, non-targeting siRNA control, E5-E8, individual siRNAs, Epool, pooled treatment using E5-E8 in equal amounts to create the same total concentration of siRNA; biological replicate experiments were performed, using primary keratinocytes from 5 different skin donors.

b. Western blot

c. Bar chart showing mean capacitance measured on the surface of skin organoid samples using a Corneometer (Courage-Khazaka Electronic, Köln); error bars show standard deviation; C4, non-targeting siRNA control, E5-E8, individual siRNAs, Epool, pooled treatment using E5-E8 in equal amounts to create the same total concentration of siRNA; biological replicate experiments were performed, using primary keratinocytes from 3 different skin donors.

d. H&E stained secHons of skin organoid samples Histological sections showing appearance of organoid samples untreated (mock) and treated with control (non-targeting siRNA), individual EMSY-siRNAs (E5, E6, E7, E8) and the pool of these four siRNAs in equal amounts to make the same concentration; similar findings were replicated in a total of three donors.

Figure E4. Time course showing organoid development and measurements of barrier formation

a. H&E staining of skin organotypic cultures Time after lifting culture to the air-liquid interface

b. Measurement of barrier function Water content of stratum corneum, measured using corneometer Transepidemal water loss (TEWL), measured using Aquaflux (Biox, London, UK)

c. Lucifer yellow dye penetration Time after lifting culture to the air-liquid interface

50ul of 1mM dye placed on surface of organotypic skin contained within a metal ring
Incubated at 37oC for 4 hours
Image and image analysis performed with Zeiss LSM710 fluorescent microscope
[Note this figure is reproduced for comparison in Fig 3C.]

Figure E5. EMSY over-expression in primary human keratinocytes leads to a reduction in markers of terminal differentiation and barrier function, consistent with changes previously reported to occur in AD.
Data shown are from 3 biological replicates (primary kera8nocytes from 3 separate donors) in which EMSY mRNA was increased 10-fold, 22-fold and 47-fold compared to GFP-empty vector-treated kera8nocytes (**Figure 2J**).

Figure E6. Mass spectrometry proteomic analysis quality control assessments.
a. Bins on the x-axis contain the log2 intensity-based absolute quantification (iBAQ, sum of intensities of tryptic peptides for each protein divided by number of theoretically observable peptides); normalised counts of the proteins in each bin are shown on the y-axis; MS2, MS3, MS5 and MS6 are biological replicate experiments from different human donors; mock, untreated control organoid; C4, non-targe1ng control treated organoid; Emsy, EMSY si-RNA treated organoid.
b. x and y axes show iBAQ intensities of samples mapped against replicate analysis; biological replicates are highly correlated (Pearson correlation coefficient ≥0.86)

Figure E7.
(a) Gene Ontology analysis of 154 proteins up-regulated in organoid skin with EMSY knock-down; results where FDR p<0.05
(b) Gene Ontology analysis of 130 proteins down-regulated in organoid skin with EMSY knock-down; results where FDR p<0.05
Biological process and molecular func1on show no significant enrichments after FDR

Figure E8. qPCR, Western blotting and immunofluorescence to test for validation of selected protein expression changes identified by mass spec analysis

Figure E9. Transmission electron microscopy images of organoid skin model with osmium staining, showing ultrastructure of stratum corneum
EMSY knock-down produces a thicker stratum corneum (SC) with an increased number of component layers, consistent with the increase in corneodesmosin detected by mass spectrometry; black arrows indicate corneodesmosomes; representa-ve images from four biological replicate experiments.
[Note: These upper two Images are reproduced here from Figure 2F, to allow comparison with replicate experiment.]

Figure E10. Immunohistochemistry to investigate EMSY expression in skin

ACCEPTED MANUSCRIPT

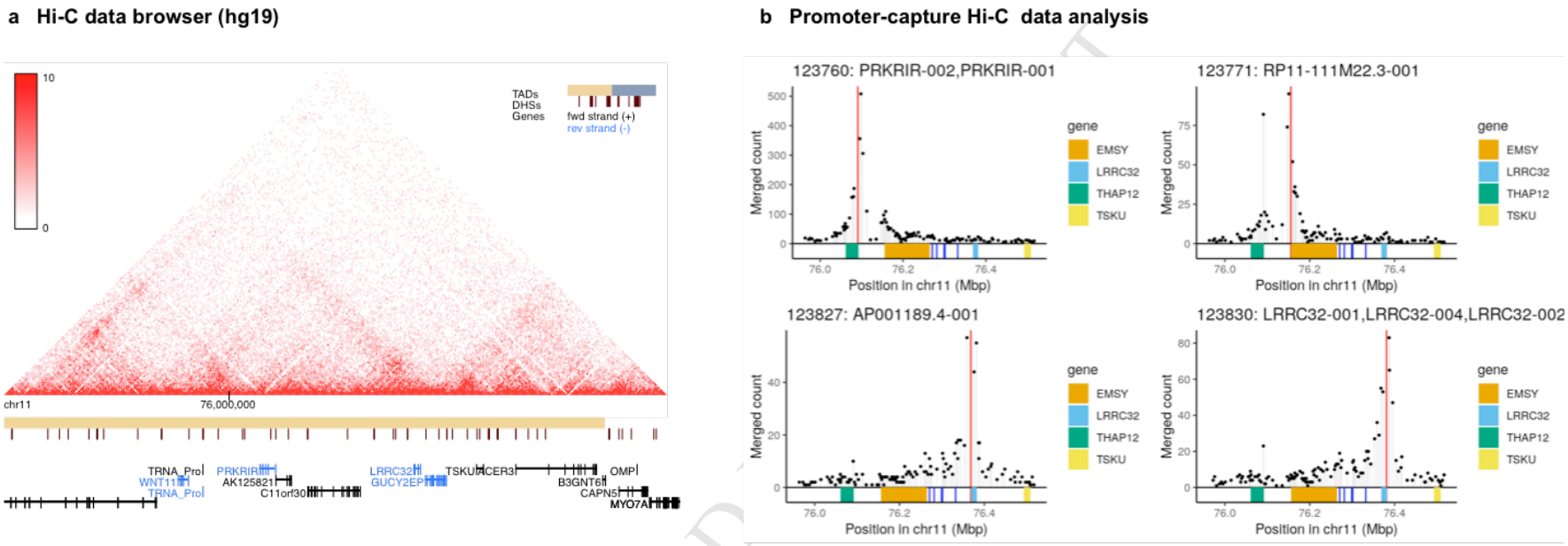
SUPPLEMENTARY FIGURES AND TABLES

EMSY expression affects multiple components of skin barrier with relevance to atopic dermatitis

Martina S Elias PhD,[1]* Sheila C Wright HNC,[1] Judit Remenyi PhD,[1] James C Abbott PhD[2], Susan E Bray PhD[3], Christian Cole PhD[2], Sharon Edwards MBChB[4], Marek Gierlinski PhD[2], Mateusz Glok[1], John A McGrath FRCP[5], William V Nicholson PhD[1], Lavinia Paternoster PhD[6], Alan R Prescott PhD[7], Sara Ten Have PhD[8], Phillip D Whitfield PhD[9], Angus I Lamond PhD[8] and Sara J Brown FRCPE[1,10]*

ACCEPTED MANUSCRIPT

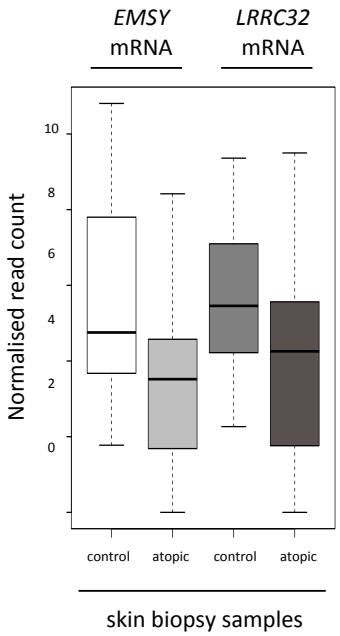
Fig E1. Chromosomal conformation data analysis



a. Data from Rao *et al.* (2014) generated using normal human keratinocytes, displayed in the Hi-C data browser from Yue lab, Penn State, USA http://promoter.bx.psu.edu/hi-c/view.php?method=Hi-C&species=human&assembly=hg19&source=inside&tissue=NHEK&type=Lieberman-raw&resolution=5&c_url=&transfer=&gene=&chr=chr11&start=75553333.333333&end=76871666.666667&sessionID=&browser=none

b. Data from Rubin *et al.* (2017) generated using normal human keratinocytes in duplicate experiments. Results are shown for day 0; cells differentiated to days 3 and 6 gave very similar results. Coloured rectangles indicate position of the genes and blue lines show the SNP positions. The vertical red line is the location of the bait. Plots shows read count added across the two replicate experiments. There is some evidence of an interaction between the SNP region and *LRRC32,* but an interaction with *EMSY* cannot be excluded.

Fig E2. Direct (single molecule) RNA sequencing of atopic skin compared to non-atopic control skin



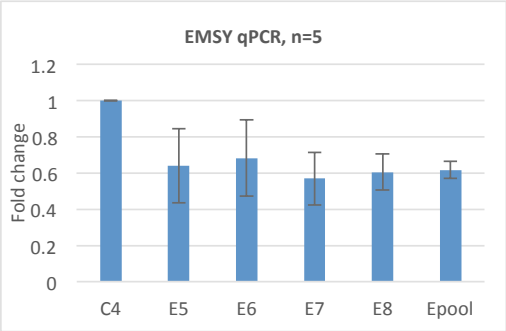
Direct RNA sequencing analysis (48) of skin biopsies from the clinically uninflamed skin of paediatric AD patients (n=26) and site-matched non-atopic control skin (n=10); box plots show median, first and third quartiles, whiskers extend to most extreme data point <1.5 x interquartile range; p>0.05

Details of the donor phenotypes and demographic details are reported in Cole *et al.* (2014).

ACCEPTED MANUSCRIPT

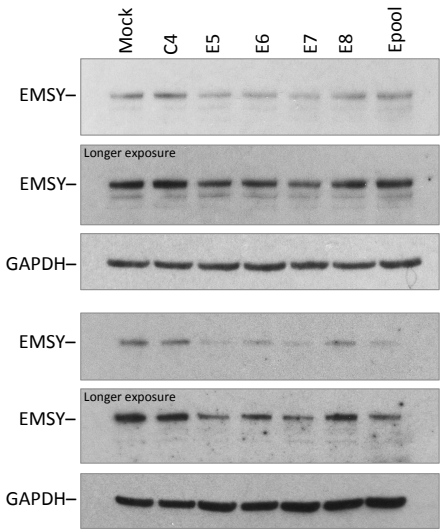
Fig E3. Comparison of effects of individual and pooled *EMSY*-siRNAs

a

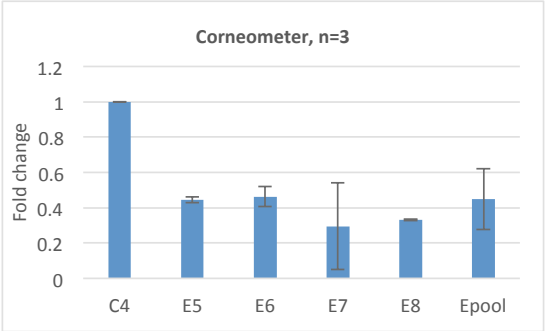


Bar chart showing mean *EMSY* mRNA; error bars show standard deviation; C4, non-targeting siRNA control, E5-E8, individual siRNAs, Epool, pooled treatment using E5-E8 in equal amounts to create the same total concentration of siRNA; biological replicate experiments were performed, using primary keratinocytes from 5 different skin donors.

b **Western blot**

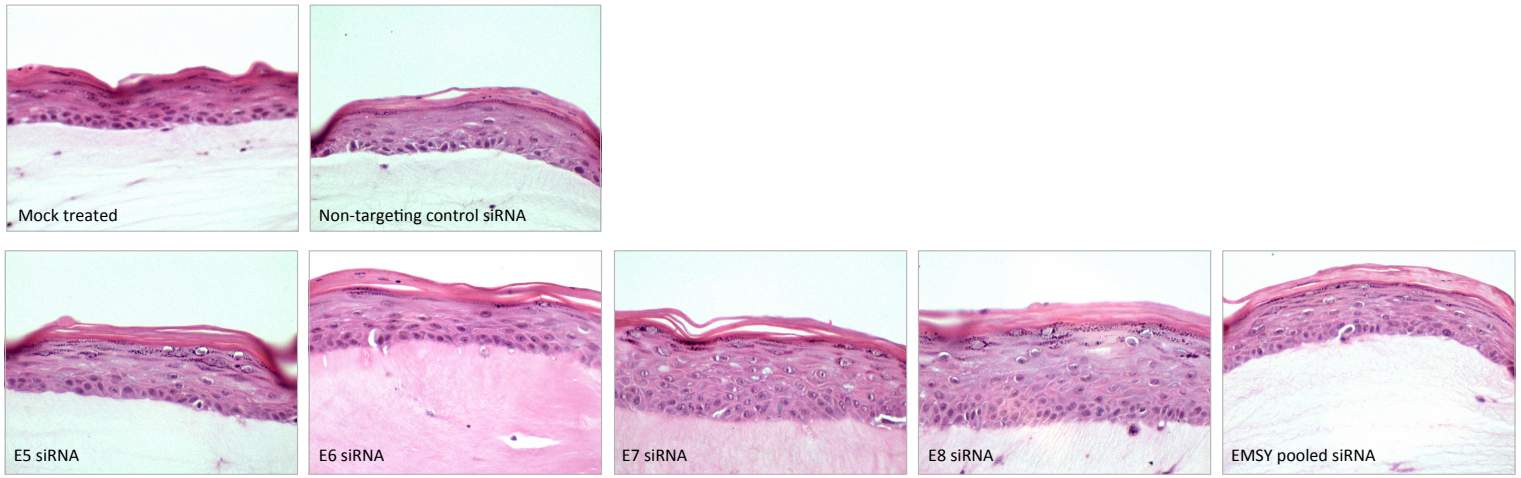


c



Bar chart showing mean capacitance measured on the surface of skin organoid samples using a Corneometer (Courage-Khazaka Electronic, Köln); error bars show standard deviation; C4, non-targeting siRNA control, E5-E8, individual siRNAs, Epool, pooled treatment using E5-E8 in equal amounts to create the same total concentration of siRNA; biological replicate experiments were performed, using primary keratinocytes from 3 different skin donors.

d **H&E stained sections of skin organoid samples**

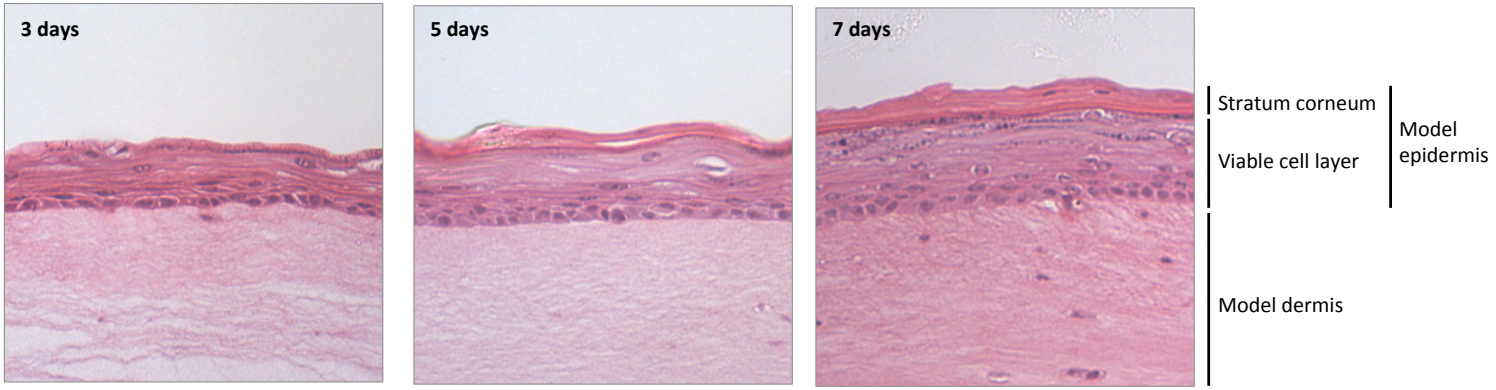


Histological sections showing appearance of organoid samples untreated (mock) and treated with control (non-targeting siRNA), individual EMSY-siRNAs (E5, E6, E7, E8) and the pool of these four siRNAs in equal amounts to make the same concentration; similar findings were replicated in a total of three donors.

Fig E4. Time course showing organoid development and measurements of barrier formation

a **H&E staining of skin organotypic cultures**

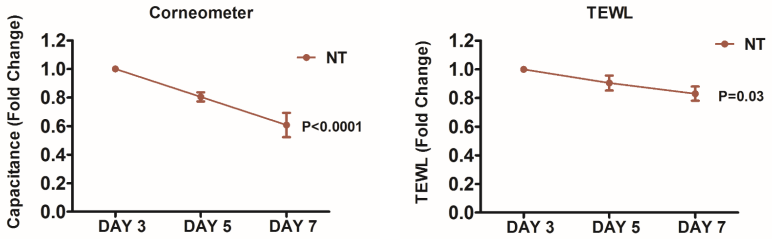
Time after lifting culture to the air-liquid interface



b **Measurement of barrier function**

Water content of stratum corneum, measured using corneometer

Transepidemal water loss (TEWL), measured using Aquaflux (Biox, London, UK)



c **Lucifer yellow dye penetration**

Time after lifting culture to the air-liquid interface

50ul of 1mM dye placed on surface of organotypic skin contained within a metal ring

Incubated at 37°C for 4 hours

Image and image analysis performed with Zeiss LSM710 fluorescent microscope

[Note this figure is reproduced for comparison in Fig 3C.]

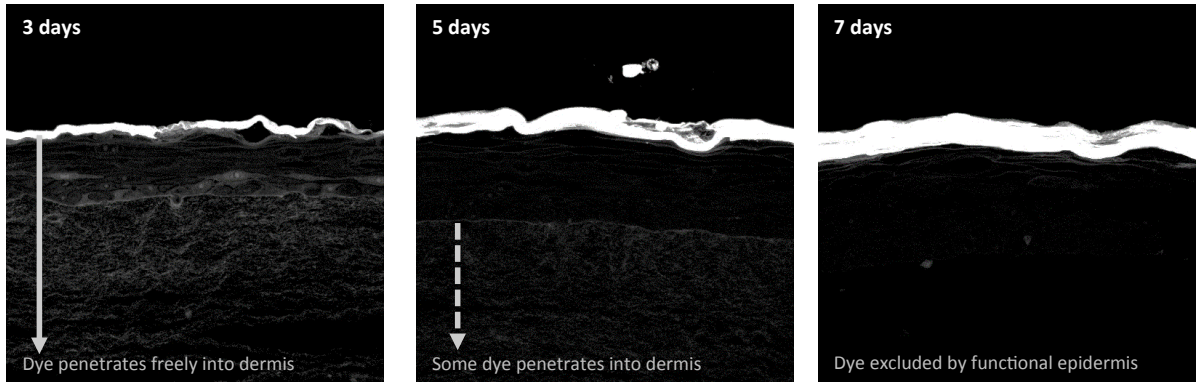
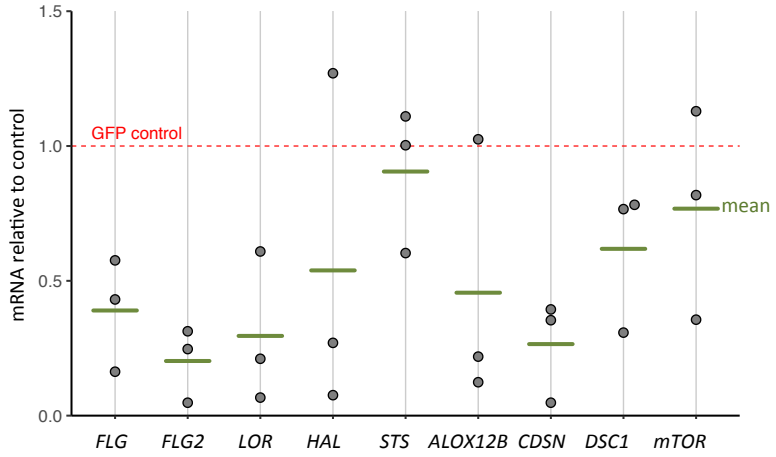


Fig E5. EMSY over-expression in primary human keratinocytes leads to a reduction in markers of terminal differentiation and barrier function, consistent with changes previously reported to occur in AD.

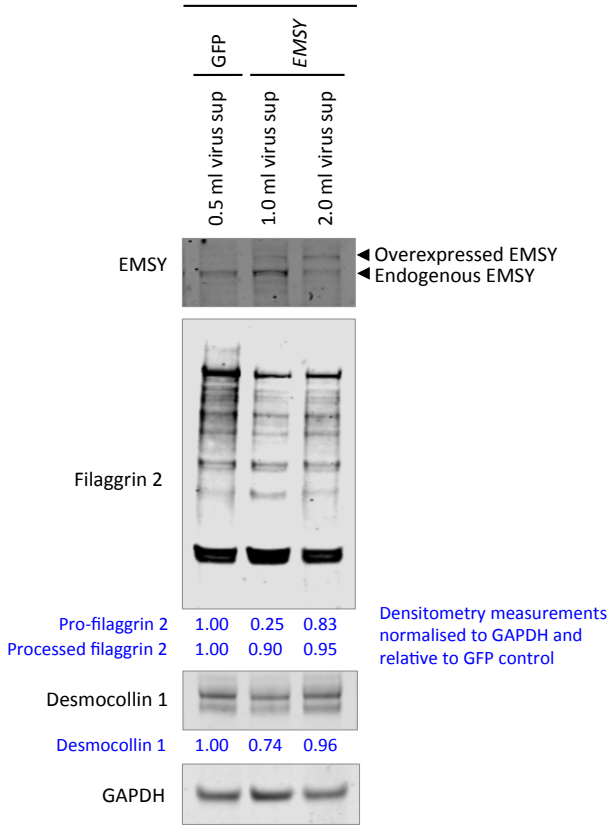
Data shown are from 3 biological replicates (primary keratinocytes from 3 separate donors) in which *EMSY* mRNA was increased 10-fold, 22-fold and 47-fold compared to GFP-empty vector-treated keratinocytes (**Figure 2J**).

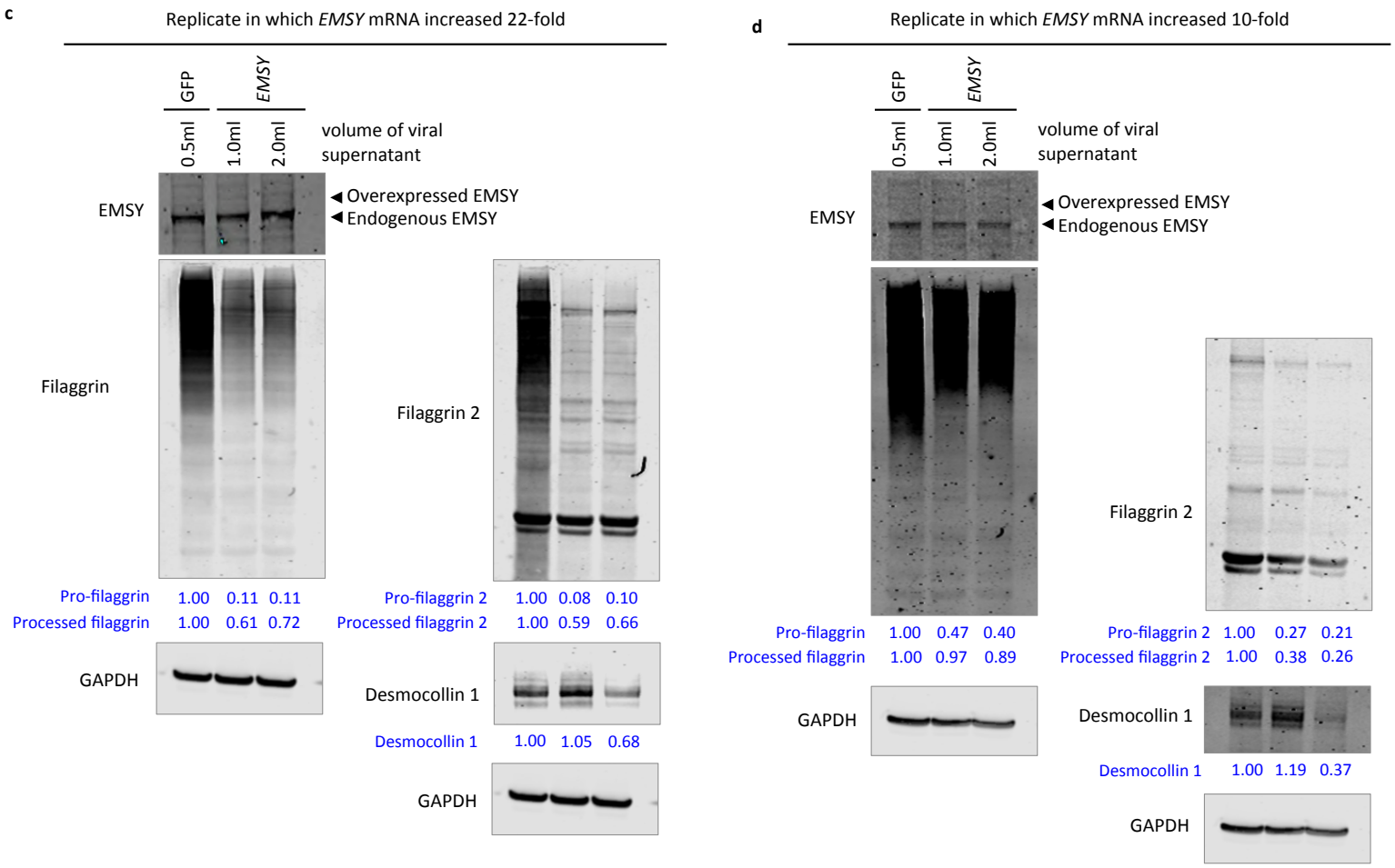
a qPCR analysis



b Western blotting

Additional results from experiment shown in **Fig. 2l-2m** in which *EMSY* mRNA increased 47-fold

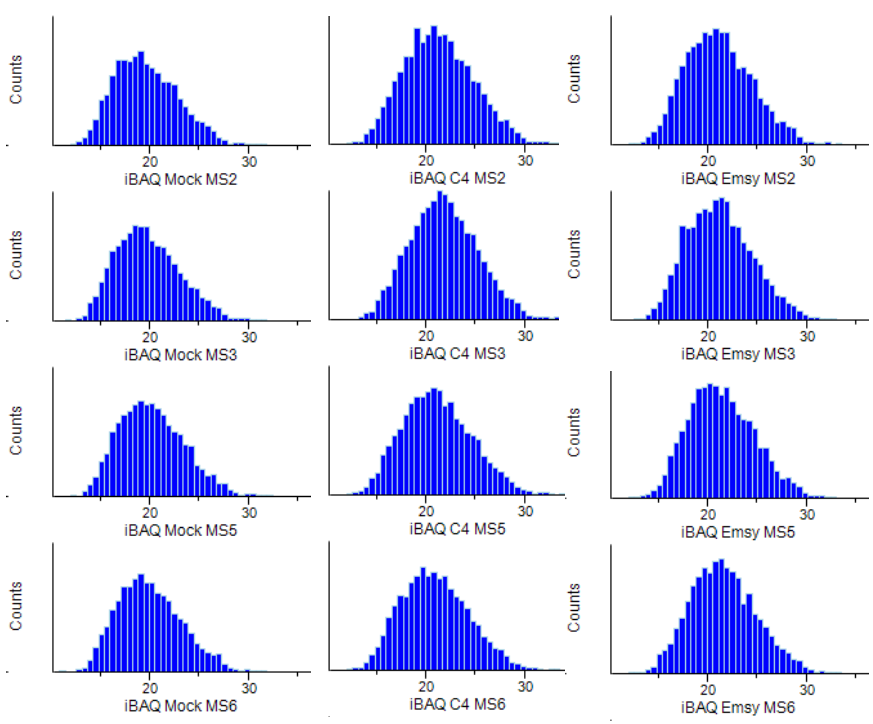




Densitometry measurements are normalised to GAPDH and relative to GFP control; ImageStudio

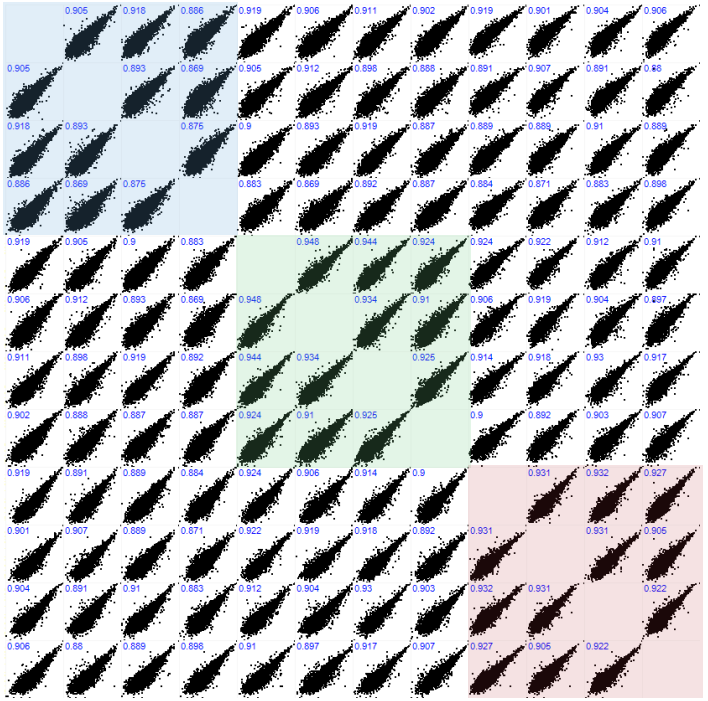
Fig E6. Mass spectrometry proteomic analysis quality control assessments.

a **Histograms showing distribution of proteins quantified in each experiment**



Bins on the x-axis contain the log2 intensity-based absolute quantification (iBAQ, sum of intensities of tryptic peptides for each protein divided by number of theoretically observable peptides); normalised counts of the proteins in each bin are shown on the y-axis; MS2, MS3, MS5 and MS6 are biological replicate experiments from different human donors; mock, untreated control organoid; C4, non-targeting control treated organoid; Emsy, EMSY si-RNA treated organoid.

b **Correlation of protein abundance from replicate analyses**



Non-targeting control

EMSY-siRNA treated

Mock-treated samples

x and y axes show iBAQ intensities of samples mapped against replicate analysis; biological replicates are highly correlated (Pearson correlation coefficient ≥0.86)

Fig E7.

(a) Gene Ontology analysis of 154 proteins up-regulated in organoid skin with EMSY knock-down; results where FDR p<0.05

Biological process

Analysis Type:	PANTHER Overrepresentation Test (Released 20181113)						
Annotation Version and Release Date:	GO Ontology database Released 2018-11-15						
Analyzed List:	upload_1 (Homo sapiens)						
Reference List:	Homo sapiens (all genes in database)						
Test Type:	FISHER						
Correction:	FDR						
GO biological process complete	Homo sapiens - REFLIST (21042)	upload_1 (161)	upload_1 (expected)	upload_1 (over/under)	upload_1 (fold Enrichment)	upload_1 (raw P-value)	upload_1 (FDR)
establishment of skin barrier (GO:0061436)	21	4	0.16	+	24.89	3.58E-05	3.14E-02
regulation of water loss via skin (GO:0033561)	23	4	0.18	+	22.73	4.90E-05	3.87E-02
cornification (GO:0070268)	112	7	0.86	+	8.17	3.51E-05	3.46E-02
cellular response to toxic substance (GO:0097237)	201	9	1.54	+	5.85	3.36E-05	3.54E-02
autophagy (GO:0006914)	245	10	1.87	+	5.33	2.63E-05	3.45E-02
process utilizing autophagic mechanism (GO:0061919)	245	10	1.87	+	5.33	2.63E-05	3.19E-02
skin development (GO:0043588)	376	12	2.88	+	4.17	4.28E-05	3.56E-02
ncRNA metabolic process (GO:0034660)	537	15	4.11	+	3.65	2.13E-05	3.06E-02
RNA processing (GO:0006396)	850	20	6.5	+	3.08	1.03E-05	2.03E-02
cell death (GO:0008219)	1073	22	8.21	+	2.68	2.90E-05	3.27E-02
programmed cell death (GO:0012501)	1038	21	7.94	+	2.64	5.41E-05	4.06E-02
cellular catabolic process (GO:0044248)	1736	30	13.28	+	2.26	3.56E-05	3.31E-02
catabolic process (GO:0009056)	1972	33	15.09	+	2.19	1.80E-05	3.15E-02
gene expression (GO:0010467)	1986	33	15.2	+	2.17	2.02E-05	3.19E-02
nucleic acid metabolic process (GO:0090304)	2293	35	17.54	+	1.99	6.72E-05	4.82E-02
cellular nitrogen compound metabolic process (GO:0034641)	3575	51	27.35	+	1.86	7.06E-06	1.59E-02
cellular metabolic process (GO:0044237)	7584	92	58.03	+	1.59	8.77E-08	6.92E-04
metabolic process (GO:0008152)	8426	100	64.47	+	1.55	2.48E-08	3.92E-04
nitrogen compound metabolic process (GO:0006807)	7148	83	54.69	+	1.52	5.38E-06	1.41E-02
cellular process (GO:0009987)	14350	136	109.8	+	1.24	3.50E-06	1.10E-02
biological_process (GO:0008150)	17700	155	135.43	+	1.14	1.99E-06	7.84E-03
Unclassified (UNCLASSIFIED)	3342	6	25.57	-	0.23	1.99E-06	1.05E-02

Molecular function

Analysis Type:	PANTHER Overrepresentation Test (Released 20181113)						
Annotation Version and Release Date:	GO Ontology database Released 2018-11-15						
Analyzed List:	upload_1 (Homo sapiens)						
Reference List:	Homo sapiens (all genes in database)						
Test Type:	FISHER						
Correction:	FDR						
GO molecular function complete	Homo sapiens - REFLIST (21042)	upload_1 (161)	upload_1 (expected)	upload_1 (over/under)	upload_1 (fold Enrichment)	upload_1 (raw P-value)	upload_1 (FDR)
RNA binding (GO:0003723)	1670	29	12.78	+	2.27	3.13E-05	3.66E-02
protein binding (GO:0005515)	11870	117	90.82	+	1.29	2.87E-05	4.48E-02
molecular_function (GO:0003674)	17654	154	135.08	+	1.14	6.77E-06	1.58E-02
Unclassified (UNCLASSIFIED)	3388	7	25.92	-	0.27	6.77E-06	3.17E-02

Cellular component

Analysis Type:	PANTHER Overrepresentation Test (Released 20181113)						
Annotation Version and Release Date:	GO Ontology database Released 2018-11-15						
Analyzed List:	upload_1 (Homo sapiens)						
Reference List:	Homo sapiens (all genes in database)						
Test Type:	FISHER						
Correction:	FDR						
GO molecular function complete	Homo sapiens - REFLIST (21042)	upload_1 (161)	upload_1 (expected)	upload_1 (over/under)	upload_1 (fold Enrichment)	upload_1 (raw P-value)	upload_1 (FDR)
RNA binding (GO:0003723)	1670	29	12.78	+	2.27	3.13E-05	3.66E-02
protein binding (GO:0005515)	11870	117	90.82	+	1.29	2.87E-05	4.48E-02
molecular_function (GO:0003674)	17654	154	135.08	+	1.14	6.77E-06	1.58E-02
Unclassified (UNCLASSIFIED)	3388	7	25.92	-	0.27	6.77E-06	3.17E-02

ACCEPTED MANUSCRIPT

(b) Gene Ontology analysis of 130 proteins down-regulated in organoid skin with EMSY knock-down; results where FDR p<0.05

Biological process and molecular function show no significant enrichments after FDR

Cellular component

Analysis Type:	PANTHER Overrepresentation Test (Released 20181113)						
Annotation Version and Release Date:	GO Ontology database Released 2018-11-15						
Analyzed List:	upload_1 (Homo sapiens)						
Reference List:	Homo sapiens (all genes in database)						
Test Type:	FISHER						
Correction:	FDR						
GO cellular component complete	Homo sapiens - REFLIST (21042)	upload_1 (132)	upload_1 (expected)	upload_1 (over/under)	upload_1 (fold Enrichment)	upload_1 (raw P-value)	upload_1 (FDR)
mitochondrial envelope (GO:0005740)	747	19	4.69	+	4.05	2.89E-07	7.36E-05
mitochondrial membrane (GO:0031966)	705	17	4.42	+	3.84	2.62E-06	4.84E-04
mitochondrial part (GO:0044429)	1042	25	6.54	+	3.82	9.14E-09	4.65E-06
mitochondrial inner membrane (GO:0005743)	472	11	2.96	+	3.72	2.25E-04	2.08E-02
Golgi membrane (GO:0000139)	753	17	4.72	+	3.6	6.15E-06	9.63E-04
Golgi subcompartment (GO:0098791)	856	18	5.37	+	3.35	8.32E-06	1.21E-03
organelle inner membrane (GO:0019866)	532	11	3.34	+	3.3	6.04E-04	4.92E-02
envelope (GO:0031975)	1190	23	7.47	+	3.08	1.63E-06	3.69E-04
organelle envelope (GO:0031967)	1190	23	7.47	+	3.08	1.63E-06	3.32E-04
mitochondrion (GO:0005739)	1595	30	10.01	+	3	5.45E-08	2.22E-05
Golgi apparatus part (GO:0044431)	972	18	6.1	+	2.95	4.36E-05	5.22E-03
Golgi apparatus (GO:0005794)	1564	23	9.81	+	2.34	1.52E-04	1.48E-02
organelle subcompartment (GO:0031984)	1708	25	10.71	+	2.33	7.42E-05	7.95E-03
cytosol (GO:0005829)	5095	66	31.96	+	2.06	2.68E-10	1.82E-07
organelle membrane (GO:0031090)	2978	37	18.68	+	1.98	4.40E-05	4.97E-03
cytoplasmic part (GO:0044444)	9710	107	60.91	+	1.76	3.73E-16	7.59E-13
cytoplasm (GO:0005737)	11571	114	72.59	+	1.57	1.97E-14	2.01E-11
intracellular organelle part (GO:0044446)	9262	85	58.1	+	1.46	3.63E-06	6.16E-04
organelle part (GO:0044422)	9563	85	59.99	+	1.42	1.46E-05	1.98E-03
intracellular membrane-bounded organelle (GO:0043231)	10966	93	68.79	+	1.35	2.30E-05	2.93E-03
intracellular (GO:0005622)	14508	117	91.01	+	1.29	2.00E-07	6.77E-05
intracellular part (GO:0044424)	14508	117	91.01	+	1.29	2.00E-07	5.80E-05
membrane-bounded organelle (GO:0043227)	12474	100	78.25	+	1.28	8.38E-05	8.53E-03
cell part (GO:0044464)	16974	122	106.48	+	1.15	2.33E-04	2.06E-02
cell (GO:0005623)	17037	122	106.88	+	1.14	0.000327	0.0278

ACCEPTED MANUSCRIPT

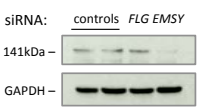
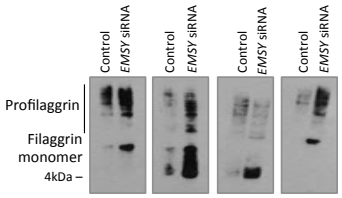
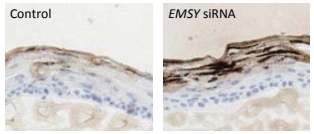
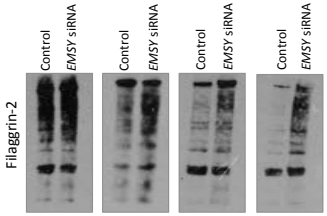
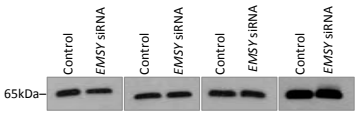
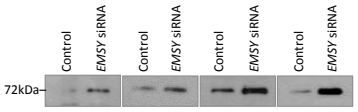
SUPPLEMENTARY FIGURES AND TABLES - continued

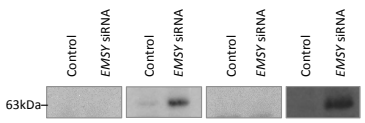
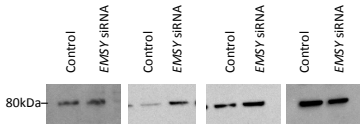
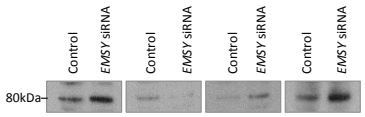
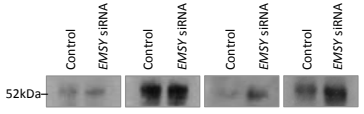
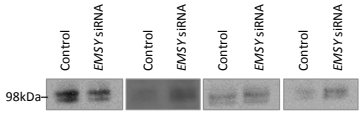
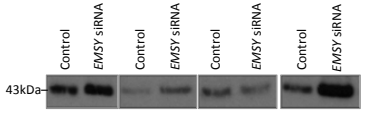
EMSY expression affects multiple components of skin barrier with relevance to atopic dermatitis

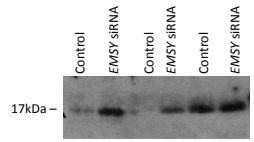
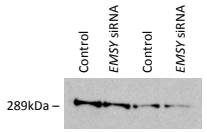
Martina S Elias PhD,[1]* Sheila C Wright HNC,[1] Judit Remenyi PhD,[1] James C Abbott PhD[2], Susan E Bray PhD[3], Christian Cole PhD[2], Sharon Edwards MBChB[4], Marek Gierlinski PhD[2], Mateusz Glok[1], John A McGrath FRCP[5], William V Nicholson PhD[1], Lavinia Paternoster PhD[6], Alan R Prescott PhD[7], Sara Ten Have PhD[8], Phillip D Whitfield PhD[9], Angus I Lamond PhD[8] and Sara J Brown FRCPE[1,10]*

ACCEPTED MANUSCRIPT

Fig E8. qPCR, Western blotting and immunofluorescence to test for validation of selected protein expression changes identified by mass spec analysis

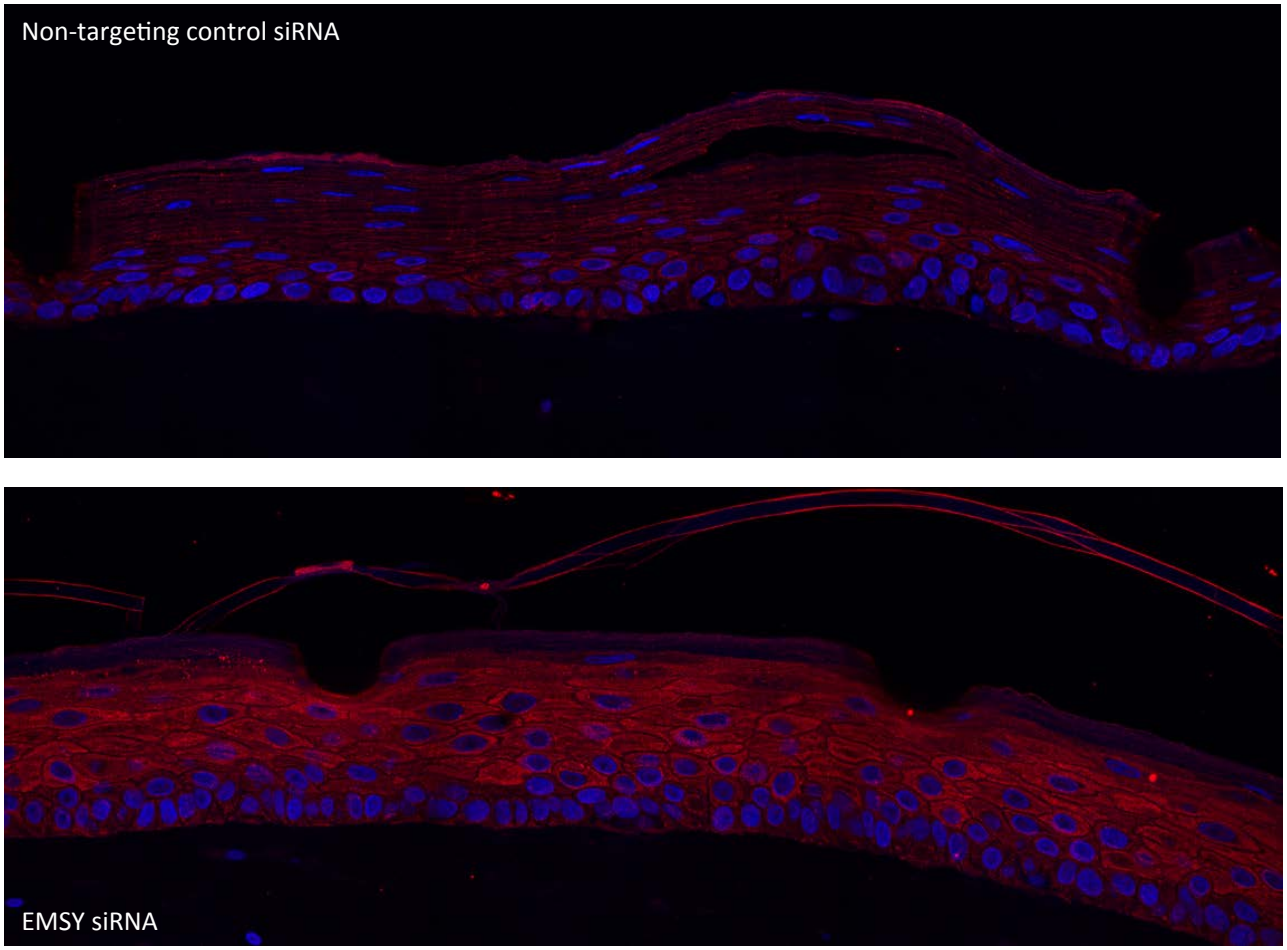
Gene	Protein	Mean FC in m/s proteomics (n=4)	Function	qPCR (fold change n=4, mean ± SEM)	Western blotting (representative images from ≥4 bio-replicates)	Immunostaining (representative images from ≥3 bio-replicates)
EMSY	EMSY	Below threshold for detection in mass spec analysis	Transcriptional regulator	0.68 ± 0.04		
FLG	Filaggrin	12.5	Structural and multifunctional	5.07 ± 4.78		
FLG2	Filaggrin 2	38.1		25.28 ± 19.57		Not done
KRT2	Keratin 2	7.9		41.90 ± 34.94		Immunofluorescence images shown following this table
HAL	Histidine ammonia lyase	11.9	Filaggrin processing	17.92 ± 14.23		Immunofluorescence images shown following this table
BLMH	Bleomycin hydrolase	5.8		8.50 ± 2.78	Not done	Not done
ASPRV1	Retroviral-like aspartic protease 1	11.8		43.92 ± 36.25	Not done	Not done

Gene	Protein	Mean FC in m/s proteomics (n=4)	Function	qPCR (fold change n=4, mean ± SEM)	Western blotting (representative images from ≥4 bio-replicates)	Immunofluorescence (representative images from ≥3 bio-replicates)
STS	Steroid sulphatase	7.3	Lipid processing and metabolism	1.25 ± 0.45		Nonspecific staining
ALOXE3	Arachidonate lipoxygenase 3	9.7		4.84 ± 1.25		Nonspecific staining
ALOX12B	Arachidonate lipoxygenase 12	7.4		5.43 ± 2.61		Immunofluorescence images shown following this table
APOE	Apolipoprotein E	3.1		1.87 ± 0.36	Not done	Not done
CDSN	Corneodesmosin	51.6	Cell-cell adhesion	56.38 ± 50.78		Immunofluorescence images shown following this table
DSC1	Desmocollin 1	7.2		2.90 ± 0.47		Immunofluorescence images shown following this table
GJA1	Gap junction alpha-1 protein (connexin 43)	2.5	Cell-cell communication	1.21 ± 0.27		Nonspecific staining

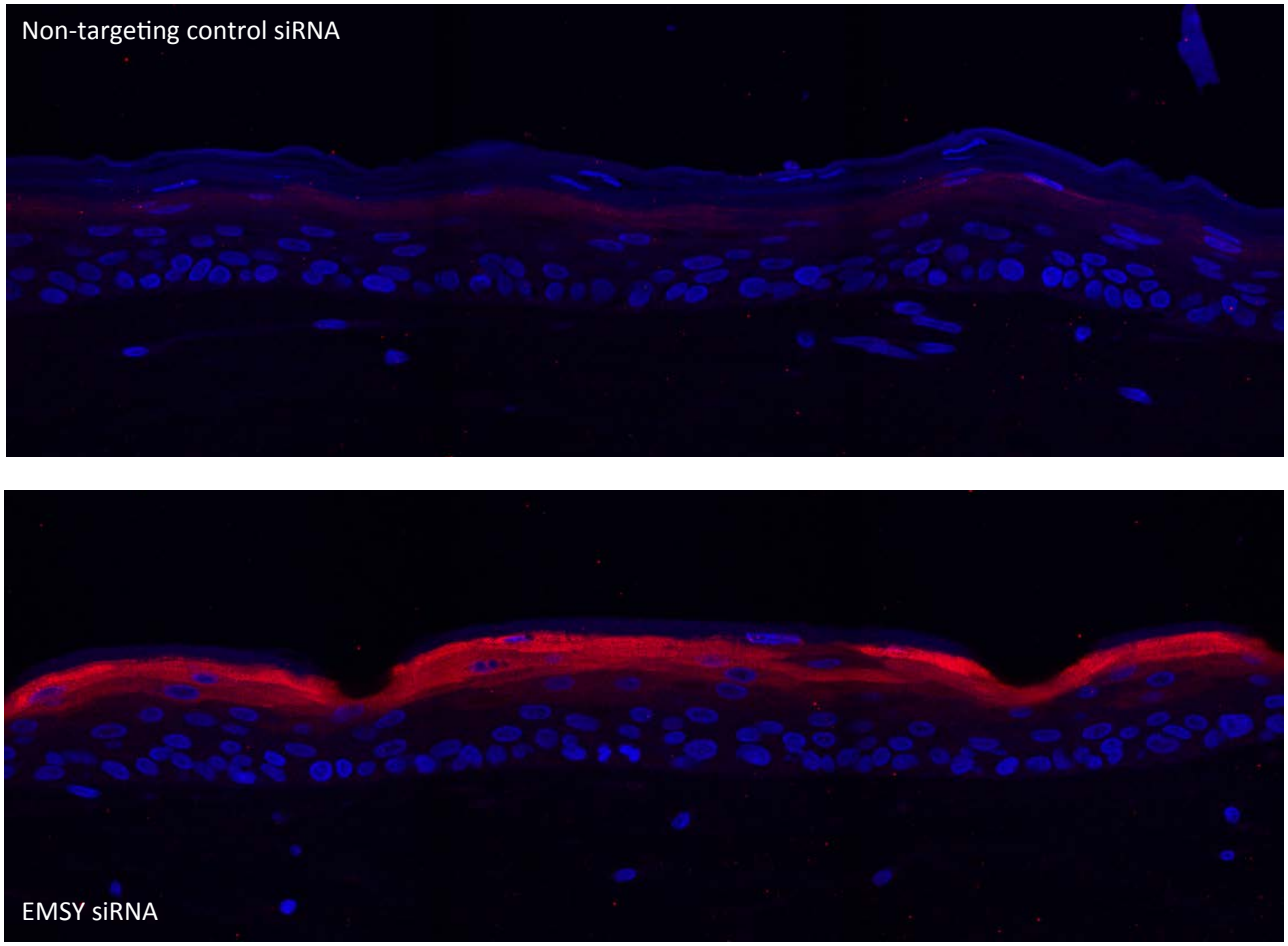
Gene	Protein	Mean FC in m/s proteomics (n=4)	Function	qPCR (fold change n=4, mean ± SEM)	Western blotting (representative images from ≥4 bio-replicates)	Immunofluorescence (representative images from ≥3 bio-replicates)
IL36RN	Interleukin-36 receptor antagonist protein	4.2	Control of inflammation	6.70 ± 4.03		Nonspecific staining
mTOR	Mechanistic target of rapamycin	0.3	Cell cycle and cell proliferation	1.36 ± 0.25		Immunofluorescence images shown following this table
CDK1	Cyclin-dependent kinase 1	6.8	Cell cycle	1.32 ± 0.21	Not done	Not done
COL7A1	Collagen alpha-1 7 chain	5.3	Basement membrane	1.46 ± 0.53	Not done	No clear staining seen
RNAse7	Ribonuclease 7	20.5	Antimicrobial	17.76 ± 15.13	Not done	Not done

ACCEPTED MANUSCRIPT

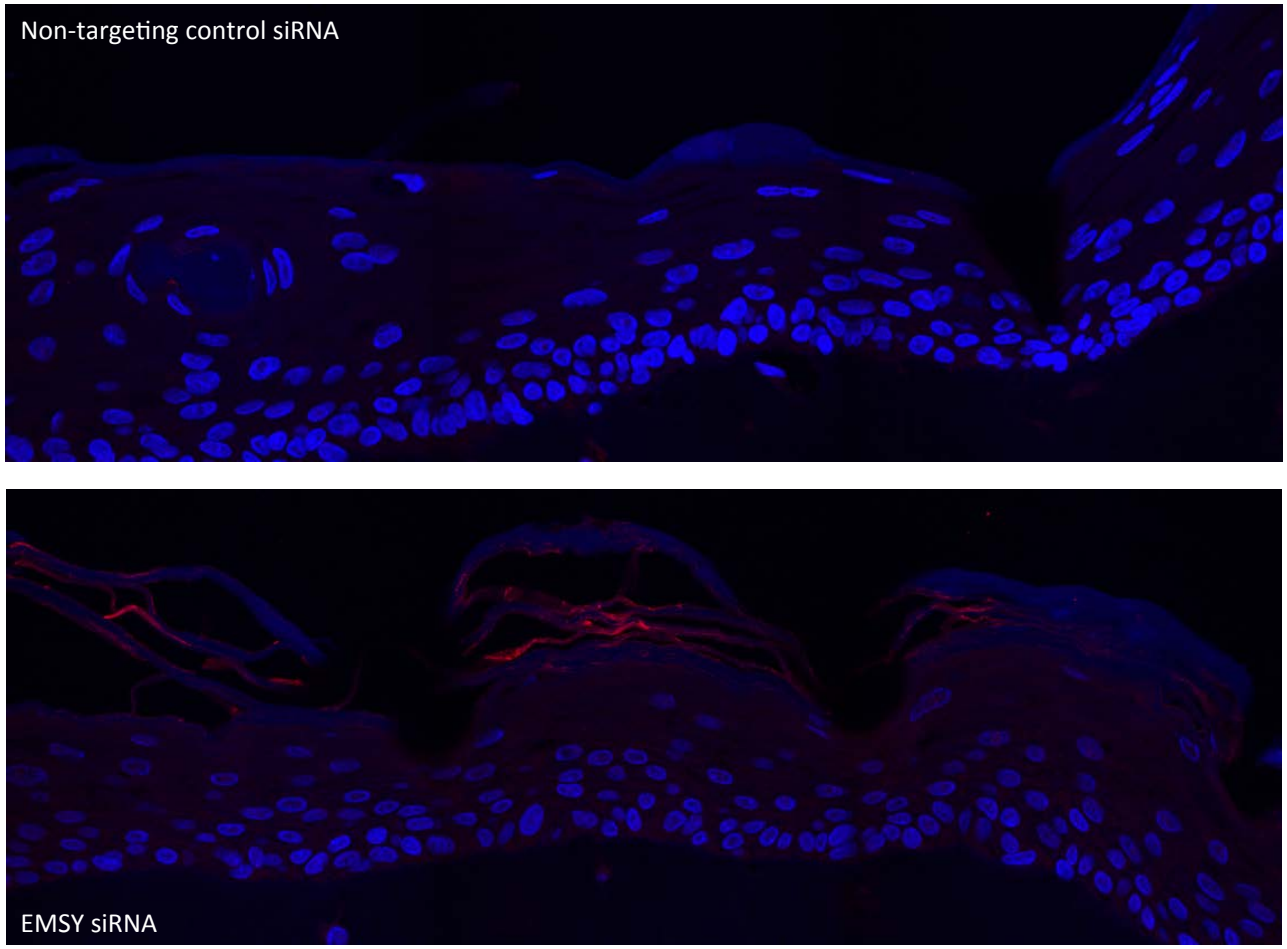
Keratin 2 DAPI
Composite image created by Zeiss LSM710 microscope



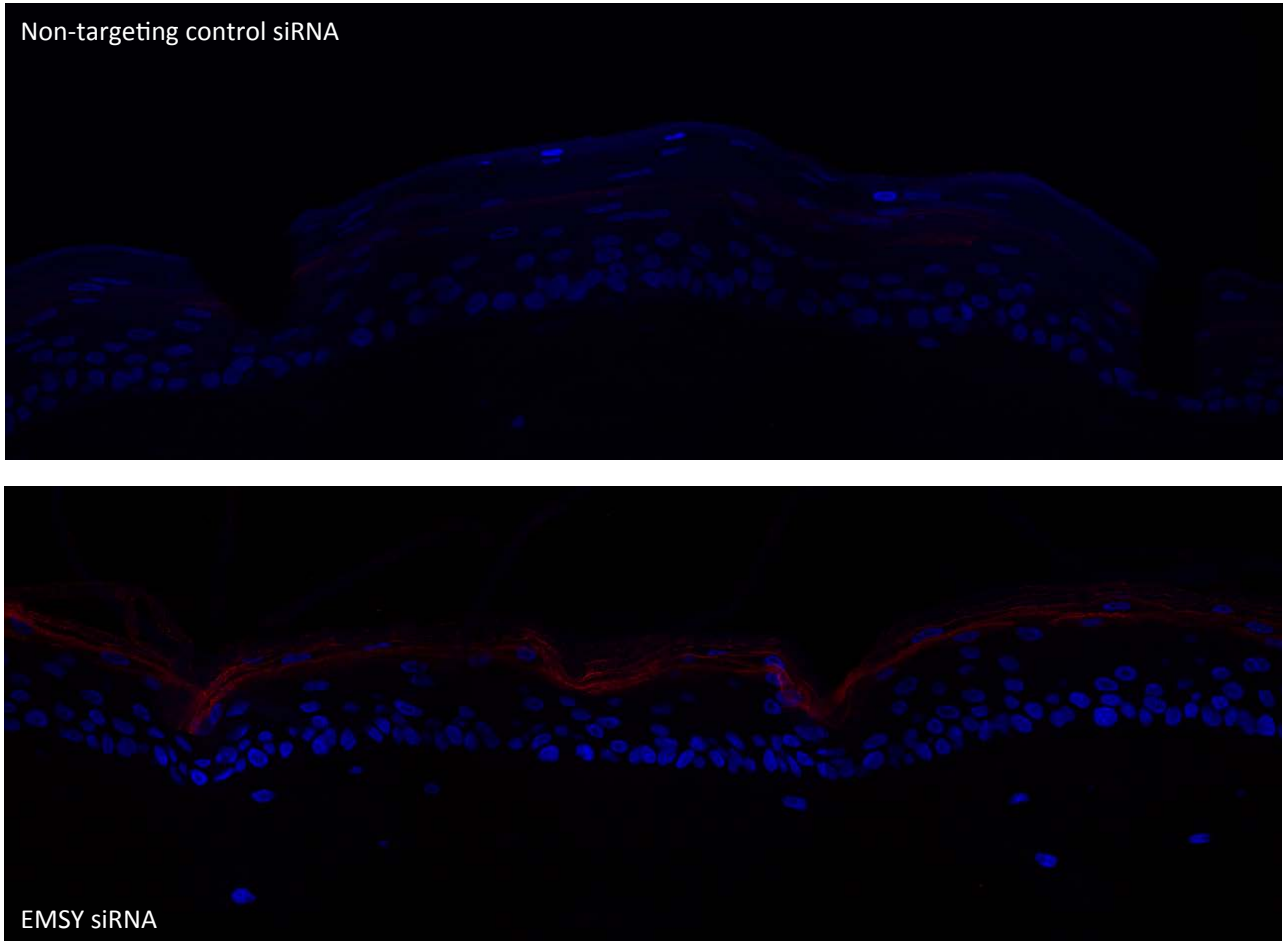
Histidine ammonia lyase DAPI
Composite image created by Zeiss LSM710 microscope



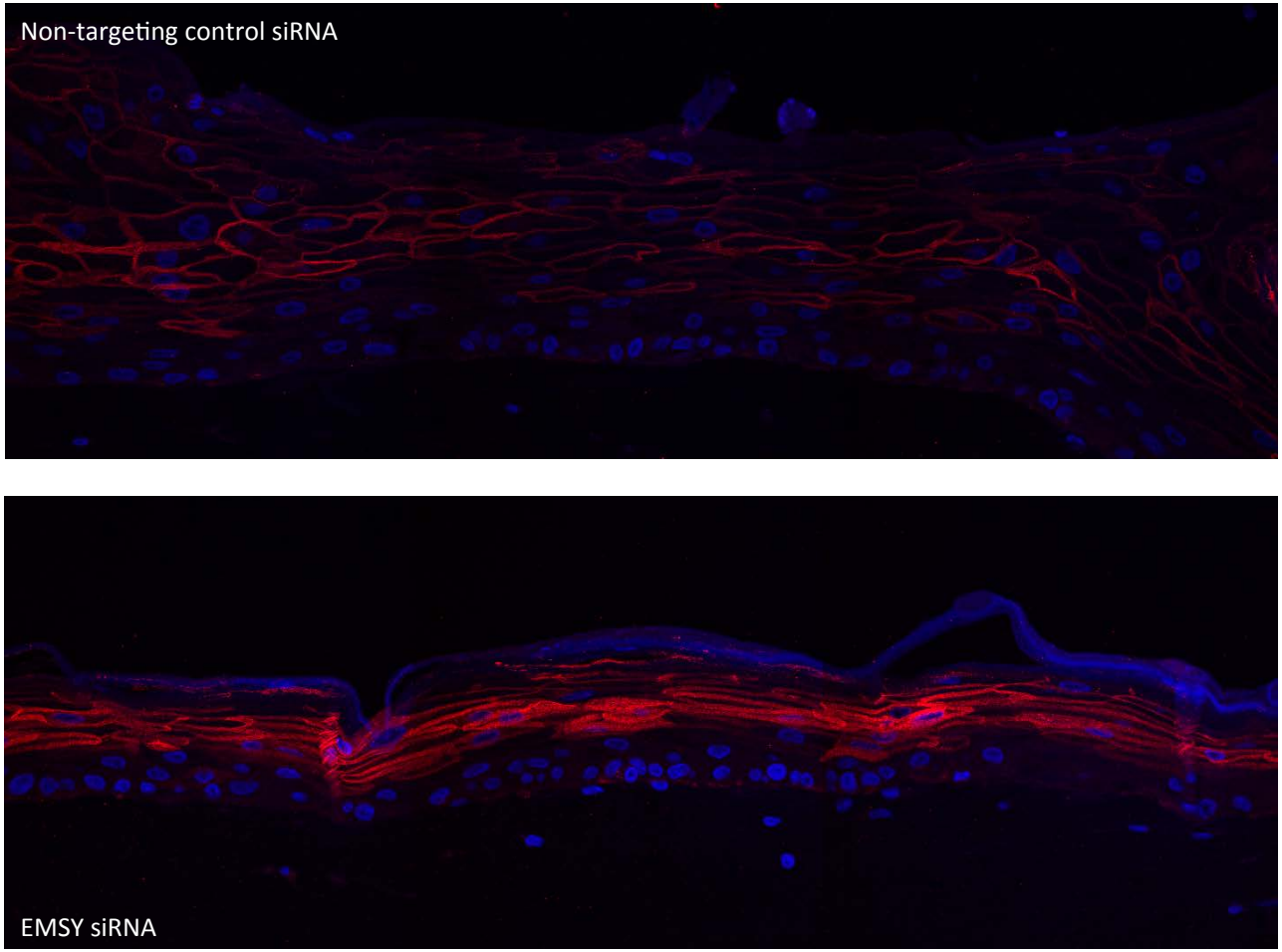
ALOX12 DAPI
Composite image created by Zeiss LSM710 microscope



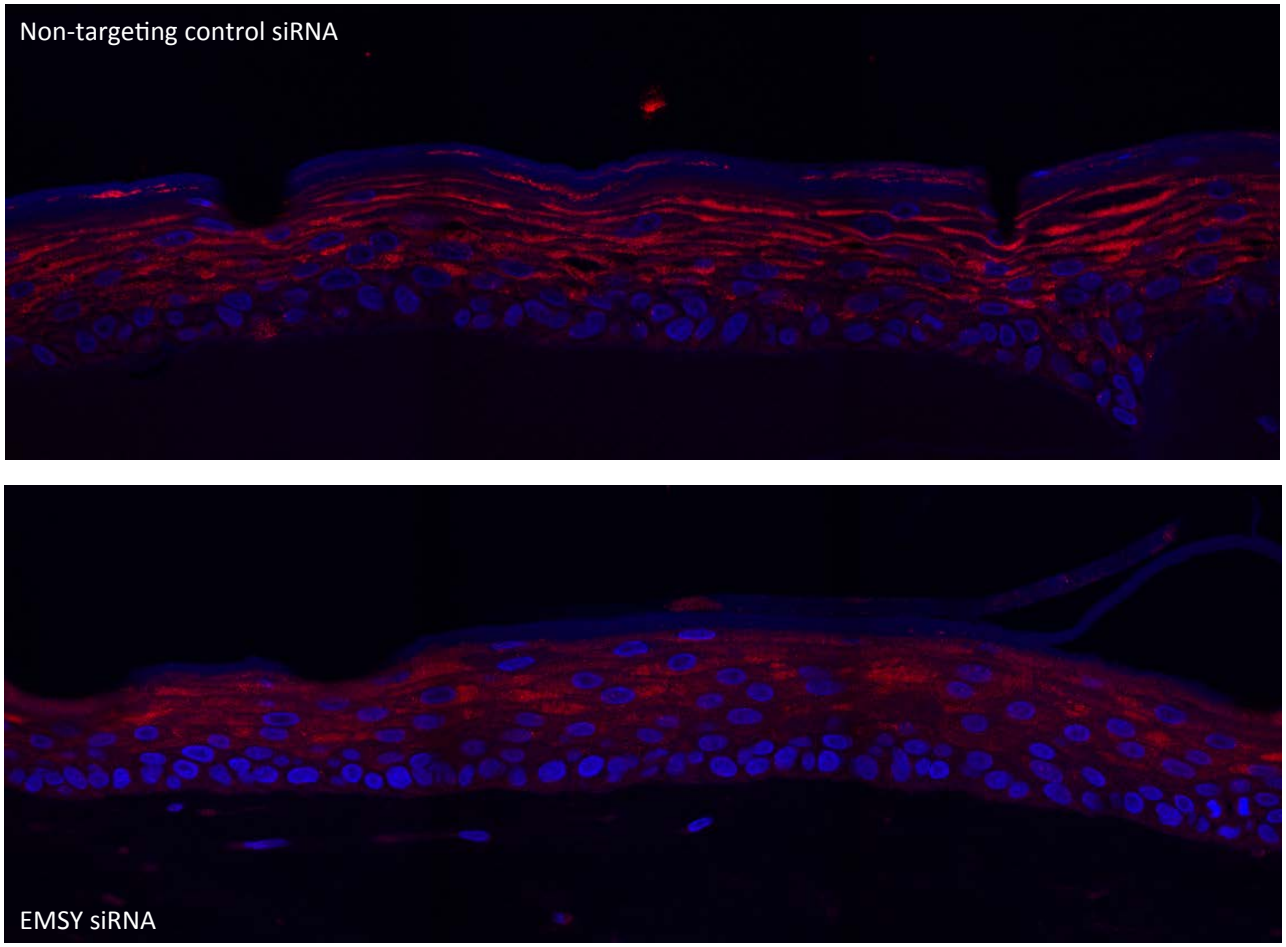
Corneodesmosin DAPI
Composite image created by Zeiss LSM710 microscope



Desmocollin DAPI
Composite image created by Zeiss LSM710 microscope



mTOR DAPI
Composite image created by Zeiss LSM710 microscope



ACCEPTED MANUSCRIPT

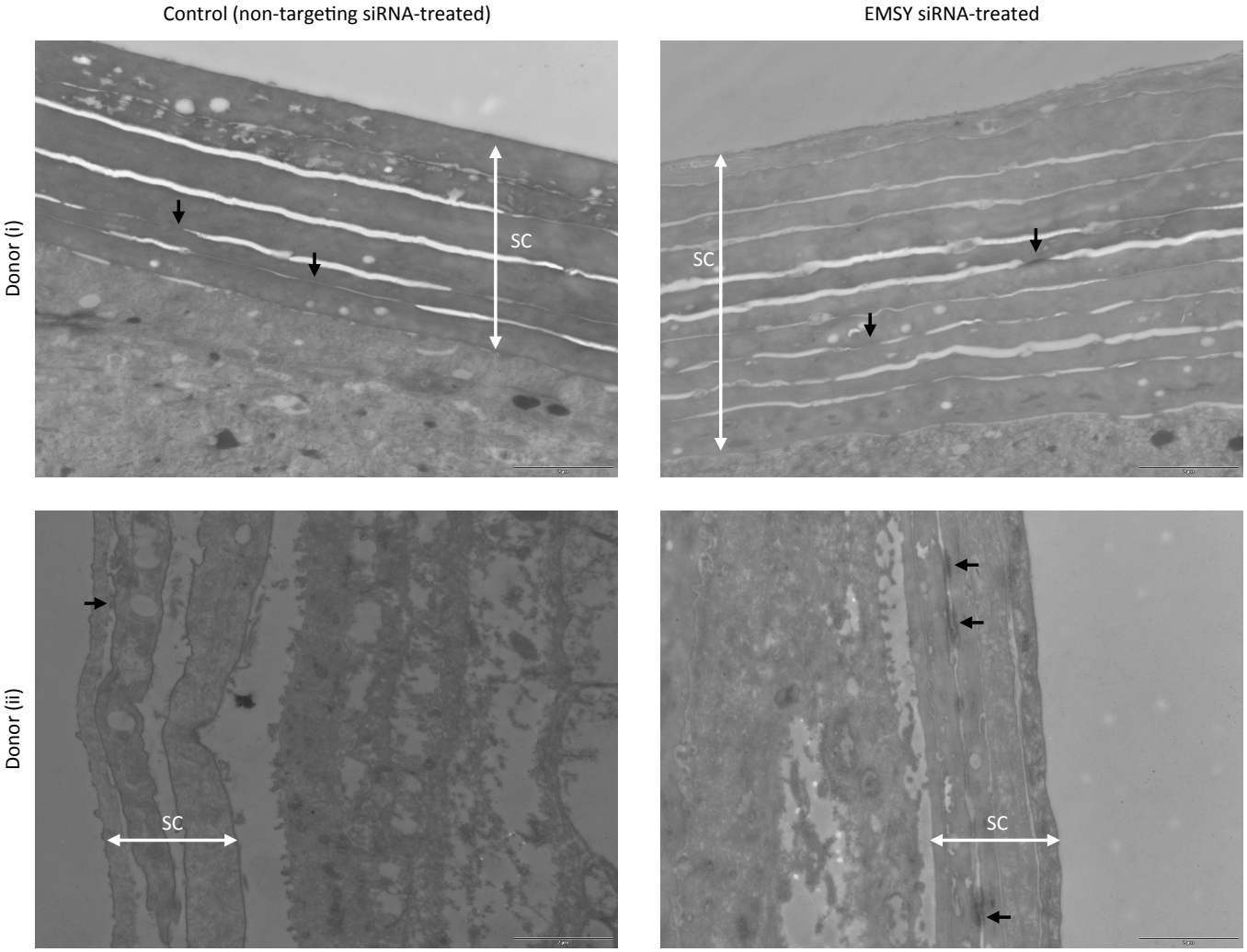
SUPPLEMENTARY FIGURES AND TABLES – continued

EMSY expression affects multiple components of skin barrier with relevance to atopic dermatitis

Martina S Elias PhD,[1]* Sheila C Wright HNC,[1] Judit Remenyi PhD,[1] James C Abbott PhD[2], Susan E Bray PhD[3], Christian Cole PhD[2], Sharon Edwards MBChB[4], Marek Gierlinski PhD[2], Mateusz Glok[1], John A McGrath FRCP[5], William V Nicholson PhD[1], Lavinia Paternoster PhD[6], Alan R Prescott PhD[7], Sara Ten Have PhD[8], Phillip D Whitfield PhD[9], Angus I Lamond PhD[8] and Sara J Brown FRCPE[1,10]*

ACCEPTED MANUSCRIPT

Fig E9. Transmission electron microscopy images of organoid skin model with osmium staining, showing ultrastructure of stratum corneum

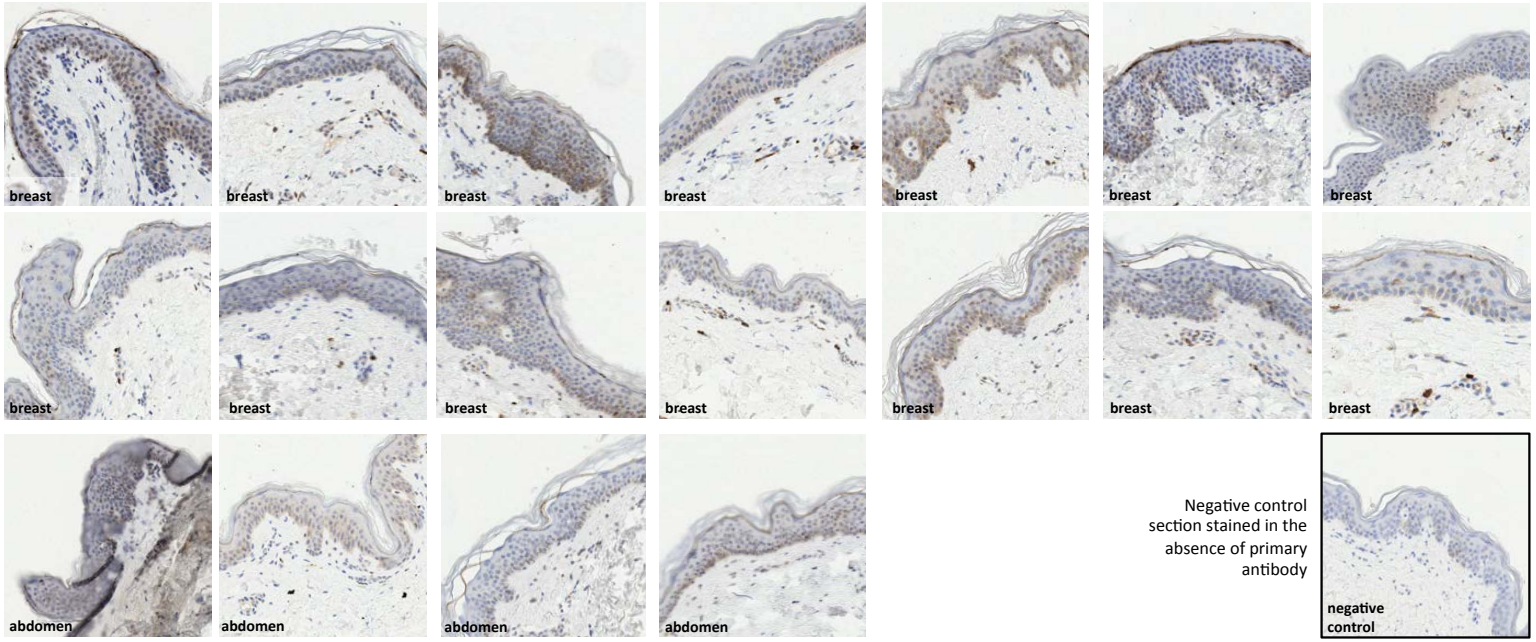


[Note: These upper two Images are reproduced here from Figure 2F, to allow comparison with replicate experiment.]

EMSY knock-down produces a thicker stratum corneum (SC) with an increased number of component layers, consistent with the increase in corneodesmosin detected by mass spectrometry; black arrows indicate corneodesmosomes; representative images from four biological replicate experiments.

Fig E10. Immunohistochemistry to investigate EMSY expression in skin

Normal control skin obtained from plastic surgical excision of breast or abdominal skin



Dermatitis cases with clinical and/or histological features of AD from different body sites as labelled

